Reducing the depth of linear reversible quantum circuits

Timothee Goubault De Brugiere, Marc Baboulin, Benoît Valiron, Simon Martiel, Cyril Allouche

IEEE Transactions on Quantum Engineering

Received May 10, 2021; accepted June 11, 2021; date of publication July 7, 2021;
date of current version August 26, 2021.

Digital Object Identifier 10.1109/TQE.2021.3091648

Reducing the Depth of Linear Reversible Quantum Circuits

TIMOTHÉE GOUBAULT DE BRUGIÈRE[1,3], MARC BABOULIN[1], BENOÎT VALIRON[2], SIMON MARTIEL[3], AND CYRIL ALLOUCHE[3]

[1] Laboratoire de Recherche en Informatique, Université Paris-Saclay, 91190 Orsay, France
[2] Laboratoire de Recherche en Informatique, CentraleSupélec, 91190 Orsay, France
[3] Atos Quantum Lab, 78340 Les Clayes-sous-Bois, France

Corresponding author: Timothée Goubault de Brugière (timothee.goubault@lri.fr).

This work was supported in part by the French National Research Agency (ANR) under the Research Project SoftQPRO ANR-17-CE25-0009-02 and in part by the Directorate General of Enterprises of the French Ministry of Industry under the Research Project PIA-GDN/QuantEx P163746-484124.

ABSTRACT In quantum computing the decoherence time of the qubits determines the computation time available, and this time is very limited when using current hardware. In this article, we minimize the execution time (the depth) for a class of circuits referred to as linear reversible circuits, which has many applications in quantum computing (e.g., stabilizer circuits, "CNOT+T" circuits, etc.). We propose a practical formulation of a divide-and-conquer algorithm that produces quantum circuits that are twice as shallow as those produced by existing algorithms. We improve the theoretical upper bound of the depth in the worst case for some range of qubits. We also propose greedy algorithms based on cost minimization to find more optimal circuits for small or simple operators. Overall, we manage to consistently reduce the total depth of a class of reversible functions, with up to 92% savings in an ancilla-free case and up to 99% when ancillary qubits are available.

INDEX TERMS Linear reversible circuits, quantum computation, reversible logic.

I. INTRODUCTION

Quantum computing is getting closer to the moment when it will be able to solve problems insoluble using current computers: the manipulation of qubits is increasingly controlled, quantum gates are performed with better fidelity, and works for achieving quantum supremacy have been proposed [1], [2], even though the significance of such works remains highly debated [3], [4].

In addition to the noise inherent in manipulating qubits, there is another phenomenon to control: quantum decoherence. The qubits must remain isolated from the outside world during the execution of the algorithm, or else they may interact unintentionally with external elements, which would distort the results. It is still difficult to isolate these qubits for a long time. If a hardware improvement is possible, it is also possible to compress the set of instructions so that their execution takes less time. These instructions are usually represented by a quantum circuit and, assuming that two nonoverlapping gates can be executed in parallel, the execution time of the circuit is strongly related to its depth. Thus, the proper execution of complex algorithms can be significantly facilitated by optimizing the depth of quantum circuits.

In a fault-tolerant computational model, the T gate is the most expensive gate to implement [5]. As a consequence, during these last years a lot of effort has been made to minimize this resource, whether it is the T-count [6]–[9] or the T-depth [10]. However, these optimizations often come with an increase of other resources, especially the number of controlled-NOT gates (CNOTs) or the total depth of the circuit. Such an additional cost is not negligible and can affect the final outputs of a quantum algorithm; see [11] for more details about why the cost of a quantum circuit should not be reduced to the T-cost. It is, therefore, important to minimize the secondary resources as well, if possible while keeping the T-cost unchanged.

Work in this direction has been carried out recently. It has mainly focused on the number of CNOTs but in a noisy intermediate-scale quantum (NISQ) setting. Overall, a significant decrease of the CNOT count is reported but with an increase of the T-depth [12]. With NISQ computers the T-depth is less important to optimize because the T-gate is not implemented fault-tolerantly, but for fault-tolerant computations we have to find a better compromise between the T-depth and the CNOT cost. Our goal in this article is to achieve

TABLE I Synthesis Algorithms and Theoretical Upper Bounds With the Approximate Ranges of Validity for Each Method

Method	Gaussian elimination	[14]	[15]	Our algorithm
Upper bound	$4n$	$2n$	$\mathcal{O}\left(\frac{n}{\log_2(n)}\right)$	$\frac{4}{3}n + 8\log_2(n)$
Best result for n such that	-	$n < 75$	$n > 1,345,000$	$75 < n < 1,345,000$

this better compromise by improving the depth of quantum circuits while keeping the T-depth as low as possible.

For this, we are interested in the optimization of a subclass of circuits called "linear reversible circuits." These circuits can be rewritten with only CNOT gates and have direct applications in other more complex circuit structures such as stabilizer circuits or CNOT+T circuits, two classes of circuits that have shown crucial utility in the design of efficient quantum compilers [6], [10] and error-correcting codes [13]. Hence, the synthesis of CNOT circuits occurs naturally in general quantum compilers and can be used as a first approach for optimizing general circuits.

In this article, we present two kinds of algorithms for the synthesis of linear reversible circuits. Our contributions are the following.

1) We present DaCSynth, a practical implementation of a divide-and-conquer framework that divides the synthesis into parallelizable subproblems that can be solved with several strategies.
2) We give strict upper bounds on the depth of the circuits. First we prove that, in all generality, the depth is upper bounded by $2n + 2\lceil\log_2(n)\rceil$ where n is the number of qubits. Then, we present a specific strategy that gives the upper bound $\frac{4}{3}n + 8\lceil\log_2(n)\rceil$. This is an improvement over the best algorithms in the literature for medium-sized registers (between a few hundreds and several thousands qubits; see Table I for more details).
3) We present greedy methods based on cost minimization techniques. They are complementary with DaCSynth in the sense that they are best suited for small problem sizes or best-case scenario while DaCSynth is better for large problems or worst-case operators.
4) We propose an extension to the case where encoded ancillary qubits are used.
5) We also give benchmarks of our method to support our theoretical results and compare them to state-of-the-art algorithms. In a worst case, DaCSynth provides circuits of depth smaller than n where n is the number of qubits. This improves the state-of-the-art algorithms by a factor of two. For small or best-case operators, the greedy methods provide almost optimal results.
6) Finally, we apply our algorithms to the optimization of a class of reversible functions, with and without ancillary qubits. Starting from a circuit with optimized T-depth, we resynthesize every chunk of purely CNOT circuits. We manage to consistently reduce the total depth of the circuits while keeping the T-count and the T-depth unchanged. Overall, we reduce the depth in average by 47% (58% with ancillary qubits) and up to 92% (99% with ancillary qubits).

The plan of this article is the following. In Section II, we present some background about the synthesis of linear reversible circuits. In Section III, we describe a new divide-and-conquer algorithm and give some strict upper bounds on the depth of the circuits synthesized by our method. In Section IV, we describe the greedy algorithms based on cost minimization techniques. We take into account encoded ancillary qubits in Section V. Benchmarks are given in Section VI. We discuss some future work in Section VII and we conclude in Section VIII.

II. BACKGROUND AND STATE OF THE ART

A. NOTION OF LINEAR REVERSIBLE FUNCTION

Let $\mathbb{F}_2$ be the Galois field of two elements. A Boolean function $f : \mathbb{F}_2^n \to \mathbb{F}_2$ is said to be linear if

$$f(x_1 \oplus x_2) = f(x_1) \oplus f(x_2)$$

for any $x_1, x_2 \in \mathbb{F}_2^n$ where $\oplus$ is the bitwise XOR operation. Let e_k be the kth canonical vector of $\mathbb{F}_2^n$. By linearity we can write for any $x = \sum_k \alpha_k e_k$ (with $\alpha_k \in \{0, 1\}$)

$$f(x) = f\left(\sum_k \alpha_k e_k\right) = \sum_k \alpha_k f(e_k)$$

and the function f can be represented with a column vector $\boldsymbol{\alpha} = [f(e_1), \ldots, f(e_n)]^T$ such that $f(x) = \alpha \cdot x$, where $\cdot$ stands for the scalar product on F_2^n and $(-)^T$ is the matrix-transpose operation. This easily extends to the n-input m-outputs functions $f : \mathbb{F}_2^n \to \mathbb{F}_2^m$ where f is defined by an $m \times n$ Boolean matrix A such that $f(x) = Ax$.

In the case of reversible Boolean functions, $n = m$, and we have a one-to-one correspondence between the inputs and the outputs. We then consider n-inputs n-outputs functions f for which the equation $y = f(x) = Ax$ must have a unique solution for any $y \in \mathbb{F}_2^n$. In other words 1) the matrix A must be invertible in $\mathbb{F}_2$ and 2) there is a one-to-one correspondence between the linear reversible functions of arity n and the invertible Boolean matrices of size n. This can be used to count the number of different linear reversible functions of n inputs (see, e.g., [16]). The application of two successive operators A and B is equivalent to the application of the operator product BA.

B. SYNTHESIS OF LINEAR REVERSIBLE BOOLEAN FUNCTIONS

We are interested in synthesizing general linear reversible Boolean functions into a reversible circuit, i.e., a series of elementary reversible gates that can be executed on a suitable hardware. For instance in quantum computing the CNOT is used in universal gate sets for superconducting and photonic qubits and performs the following 2-qubit operation:

$$\mathrm{CNOT}(x_1, x_2) = (x_1, x_1 \oplus x_2).$$

Clearly the CNOT gate is a linear reversible gate. It can be shown to be universal for linear reversible circuit synthesis: any linear reversible function of arity at least two can be implemented by a reversible circuit containing only CNOT gates. In this article, we aim at producing CNOT-based reversible circuits for any linear reversible functions.

In terms of matrices, a CNOT gate controlled by the line j acting on line $i \neq j$ can be written $E_{ij} = I + e_{ij}$ where I is the identity matrix and e_{ij} the elementary matrix with all entries equal 0 but the component (i, j) of value 1.

Generally the synthesis of an operator is done by reducing it to the identity operator. In our case, we want to compute a sequence of N elementary matrices such that

$$\prod_{k=1}^{N} E_{i_k,j_k} A = I.$$

Finally, using the fact that $E_{ij}^{-1} = E_{ij}$, we get

$$A = \prod_{k=N}^{1} E_{i_k,j_k}$$

and a circuit implementing A is given by concatenating the CNOT gates with control j_k and target i_k.

This can be generalized to the case where we allow both left and right multiplication by elementary matrices and the possibility to permute the rows and columns of A before and after the reduction to the identity operator. In other words, we look for two sequences of elementary matrices (of size N_1 and N_2) and three permutation matrices P, P_1, P_2 such that

$$\prod_{k=1}^{N_1} E_{i_k,j_k} P_1 A P_2 \prod_{k=1}^{N_2} E_{i_k,j_k} = P.$$

Even with such generalization, it is still possible to rearrange the product to write

$$A = P' \times \prod_{k=1}^{N} E_{i_k,j_k}$$

where $N = N_1 + N_2$ and P' is a permutation matrix. We read this as a CNOT circuit followed by a qubit permutation.

Left-multiplying the operator A by E_{ij} performs an elementary row operation

$$r_i \leftarrow r_i \oplus r_j$$

writing r_k for the kth row of A. Similarly, right-multiplying the operator A by E_{ij} performs an elementary column operation

$$c_j \leftarrow c_i \oplus c_j$$

writing c_k for the kth row of A.

Thus, synthesizing a linear reversible function into a CNOT-based reversible circuit is equivalent to transforming an invertible Boolean matrix A to the identity by applying elementary row and column operations. For the rest of this article, we will consequently privilege this more abstract point of view because it gives more freedom and often appears clearer for the design of algorithms. We note by $\mathrm{Row}(i, j)$ the elementary row operation $r_j \leftarrow r_i \oplus r_j$ and $\mathrm{Col}(i, j)$ the elementary column operation $c_j \leftarrow c_i \oplus c_j$.

In order to evaluate the quality of a synthesis of a linear reversible circuit a couple of metrics can be considered. The size of the circuit given by its number of CNOT gates is a first one: this gives the total number of instructions the hardware has to perform to execute the circuit. Due to the presence of noise when executing every logical gate, it is of interest to have the shortest circuit possible. In this article, we focus on the second metric, which is the depth of the circuit, i.e., the number of time steps the hardware needs to execute the circuit if we suppose that nonoverlapping gates are executed simultaneously. The depth is closely related to the execution time of the circuit. In quantum computing, the time available to perform computations is limited due to the short decoherence time of the qubits. Therefore, it is crucial to be able to produce shallow circuits for complex algorithms.

C. STATE OF THE ART

In this article, we focus on improving the depth of linear reversible circuits with a full qubit connectivity, meaning that any CNOT gate between any pair of qubits can be done—equivalently this means that any row operation is available. Recently an algorithm that produces asymptotically optimal circuits in $O(n/\log_2(n))$ was proposed [15]. The theoretical depth is given approximately by the formula

$$d = \alpha \frac{n}{\log_2(n)} + \beta \sqrt{n} \log_2(n).$$

A detailed description of the algorithm is given in Appendix B, where we estimate α and β both to 20. Thus, for practical values of n this algorithm does not provide shallow circuits.

To our knowledge, for practical register sizes, four algorithms were designed. Three of them provide similar results: the standard Gaussian elimination algorithm, the skeleton circuits in [17], and a practical algorithm proposed in [15]. All give circuits for which the depth is upper bounded by $4n$. Kutin *et al.* [14] proposed an algorithm for computing linear reversible circuits for the linear nearest neighbor architecture (LNN) in a depth of at most $5n$. In Appendix A, we describe this algorithm and we show that it can actually be extended straightforwardly to an algorithm for a full qubit connectivity

and the depth of the output circuits is upper bounded by $2n$. To our knowledge, this algorithm then is the best algorithm when the number of qubits does not exceed a few thousands.

D. OUR CONTRIBUTIONS

We exploit the promising idea developed in [15] to use a divide-and-conquer method in order to produce shallow circuits for reasonable sizes of registers. First, we show that synthesizing an operator via a divide-and-conquer algorithm is equivalent to zeroing binary matrices with a given set of elementary operations. This provides a general framework, DaCSynth, giving another view of the problem from which new strategies can be applied. The algorithm in [15] can be regarded as one particular strategy for this framework. Although not the goal of this article, this means that we can recover the asymptotic optimal behavior of their algorithm.

We propose two strategies to solve this new problem: the first one—essentially theoretical—is a block algorithm and gives improved upper bounds on the total depth in the worst case. The second algorithm is a greedy one and aims at producing the shallowest circuits possible such that they can be executed on a quantum hardware in a near future. Overall, our first algorithm produces circuits whose depth is bounded by $\frac{4}{3}n + 8\lceil \log_2(n) \rceil$, where n is the number of qubits, improving the result in [14] and [15] for intermediate sized problems. A summary of the theoretical results of the different algorithms is given in Table I. The benchmarks show that our second algorithm improves the actual depth by a factor of two compared to the extension of Kutin *et al.*'s algorithm and synthesizes circuits of depth n in the worst case.

We also study the use of purely greedy algorithms. The global idea is to use cost minimization techniques with different cost functions to find "quickly" a shallow circuit. Greedy methods generally give good results for small problem sizes or for simple operators, but at the cost of no theoretical guarantee. In our benchmarks, we will observe similar characteristics: greedy methods are the best up to a certain point where their performance degrades because they do not exploit the specific structures of the problem.

Next, we extend our framework in the case where ancillary qubits are encoded outputs of the function, i.e., we want to synthesize an operator $A_{\text{out}} \in F_2^{m\times n}$ with $m > n$ with an input operator $A_{\text{in}} \in F_2^{m\times n}$. We propose a simple block algorithm and we show that the depth increases logarithmically with the number of ancillas.

Finally we integrate our algorithms (DaCSynth and the greedy ones) into the quantum compiler Tpar [10] and test our method on a set of well-known reversible functions. This gives an overview of the total depth of quantum circuits implementing important arithmetic functions like adders, multipliers, etc.

III. ALGORITHM DACSYNTH

Given an operator $A \in F_2^{n\times n}$ to synthesize, our proposed algorithm DaCSynth is a divide-and-conquer algorithm and consists in the following steps.

1) First compute a permutation matrix P such that $PA = \begin{pmatrix} A_1 & A_2 \\ A_3 & A_4 \end{pmatrix}$ and $A_1 \in F_2^{\lceil n/2\rceil \times \lceil n/2\rceil}$ is invertible.
2) Apply row operations on A to zero the block A_3 such that the resulting matrix is $A' = \begin{pmatrix} A'_1 & A'_2 \\ 0 & A'_4 \end{pmatrix}$.
3) Apply row operations on A' to zero the block A'_2 such that the resulting matrix is $A'' = \begin{pmatrix} A''_1 & 0 \\ 0 & A''_4 \end{pmatrix}$.
4) Call recursively the algorithm on A''_1 and A''_4. When $n = 1$ return an empty set of row operations.

Step 1 is straightforward: consider the rows of the submatrix $A[:, 1 : \lceil n/2\rceil]$ (using MATLAB notation). Start from an empty set and at each step add a row to the set. If the rank of the set is increased, keep the row otherwise remove it. If the resulting set is not of rank $\lceil n/2\rceil$ this would mean that the first $\lceil n/2\rceil$ columns of A are not linearly independent, which is impossible by invertibility of A. In addition, we assume that the qubits are fully connected so we can avoid to apply P by doing a postprocessing on the circuit that would transfer the permutation operation directly at the end of the total circuit. This can be done without any overhead in the number of gates. Hence, the core of the algorithm lies in steps 2 and 3. We now give the details for processing step 2. This can be easily transposed to do step 3 as well.

Theorem 3.1: Given

$$A = \begin{pmatrix} A_1 & A_2 \\ A_3 & A_4 \end{pmatrix} \in F_2^{n\times n}$$

with $A_1 \in F_2^{\lceil n/2\rceil \times \lceil n/2\rceil}$ invertible, zeroing A_3 by applying row operations on A is equivalent to zeroing the matrix $B = A_3 A_1^{-1}$ by applying any row and column operations on B or flipping any entry of B.

Proof: First, note that by hypothesis A_1 is invertible so the matrix B does indeed exist.

1) Applying an elementary row operation $\text{Row}(i, j)$ on A_3 gives the matrix $E_{ji}A_3$ and B is updated by $E_{ji}B$. Thus, a row operation on A_3 is equivalent to a row operation on B.
2) Applying an elementary row operation $\text{Row}(i, j)$ on A_1 gives the matrix $E_{ji}A_1$ and B is updated by BE_{ji}. Thus, a row operation on A_1 is equivalent to a column operation on B.
3) B is a $\lfloor n/2\rfloor \times \lceil n/2\rceil$ matrix. The kth row of B gives the decomposition of the kth row of A_3 in the basis given by the rows of A_1. Thus, any row operation $\text{Row}(k_1, \lceil n/2\rceil + k_2)$ on A will flip the entry (k_2, k_1) of B.

With these three types of operations available on B, the invertibility of A_1 is preserved. Thus, when B is zero necessarily A_3 is also zero. ■

Obviously flipping all the 1-entries of B is enough to reduce A_3 to the null matrix, but we are concerned with the shallowest way of doing this. In the following, we show how to compute the optimal depth of the circuit zeroing B using only the flipping operation.

Theorem 3.2: With the same notations, let k be the maximum number of 1-entries in one row or one column of B. Then, if we use only the flipping operation we need a circuit of depth k to zero B.

Proof: We exploit a theoretical result about bipartite graph already used in [15]. Consider the bipartite graph $G = (V_1, V_2, E)$ where each vertex of V_1 is a row of A_1, each vertex of V_2 is a row of A_3, and B is the adjacency matrix of G. Any matching in G represents a series of row operations that can be executed in parallel and that will zero some entries in B. If there is at most k nonzero entries in each row and column of B this means that the degree of G is k as well. Any bipartite graph of degree d can be decomposed into exactly d matchings [18]. Hence, a circuit of depth k is needed to transform B into the null matrix. ■

We are now able to give a strict upper bound on the worst case result of the algorithm DaCSynth.

Corollary 3.2.1: The depth of the circuits given by the algorithm DaCSynth is upper bounded by $2n + 2\lceil \log_2(n) \rceil$ with n the number of qubits.

Proof: A first straightforward formula for the depth of the circuit output by the algorithm DaCSynth is

$$d(n) = d(\lceil n/2 \rceil) + 2 \times d^*(\lceil n/2 \rceil)$$

where d^* is the depth of the circuits computing parts 2 and 3. Using the result of the previous theorem, we have

$$d^*(n) \leq n.$$

So overall the depth of our circuit is upper bounded by

$$d(n) \leq d(\lceil n/2 \rceil) + 2\lceil n/2 \rceil.$$

As $d(1) = 0$ and by exploiting the fact that $\lceil \lceil n/2 \rceil / 2 \rceil = \lceil n/4 \rceil$, we have

$$d(n) \leq 2 \times \left(\sum_{k=1}^{\lceil \log_2(n) \rceil} \lceil n/2^k \rceil \right) \leq 2 \times \left(\sum_{k=1}^{\lceil \log_2(n) \rceil} n/2^k + 1 \right).$$

After simplification, we have

$$d(n) \leq 2n + 2\lceil \log_2(n) \rceil.$$

■

A. BLOCK ALGORITHM FOR STEPS 2 AND 3

In order to improve the upper bound of our framework, we propose a block method for performing steps 2 and 3. Given an $n \times n$ matrix B to zero and an integer $k < n$ such that $n = bk + r$, we divide B into a matrix of $\lceil \frac{n}{k} \rceil \times \lceil \frac{n}{k} \rceil$ blocks as follows:

1) $\lfloor \frac{n}{k} \rfloor^2$ are of size k;
2) $\lfloor \frac{n}{k} \rfloor$ are of size $k \times r$;
3) $\lfloor \frac{n}{k} \rfloor$ are of size $r \times k$;
4) the lower right one is of size $r \times r$.

If B is of size $n \times (n+1)$ or $(n+1) \times n$ (which can happen if A is of odd size) then some blocks on the edge will be of size $k \times (r+1)$ or $(r+1) \times k$. In any case as $r < k$ then $r + 1 \leq k$ and the critical point is that all of these rectangular blocks are smaller than the $k \times k$ blocks.

Now we consider each nonzero block as a 1-entry in a $\lceil \frac{n}{k} \rceil \times \lceil \frac{n}{k} \rceil$ binary matrix that can be mapped to a bipartite graph G as above. Then, it is clear that a matching in G corresponds to a subset of blocks on which we can apply row and column operations in parallel.

Considering one such matching, we assume that we can reduce the maximum number of one-entries in each row and column of one block to an integer p in depth at most D. Then, all the blocks are matrices with at most p nonzero entries per row and column and we can flip all of these nonzero entries in p sequences of row operations as they belong to different rows and columns in B. After that all the blocks of the matching are zero and we can repeat the process with another matching without modifying the nullified blocks. G can be decomposed into at most $\lceil \frac{n}{k} \rceil$ matchings, each of them requires a depth of at most $D + p$ to zero all the blocks so the total depth for performing step 2 (or step 3) is $(D + p) \times \lceil \frac{n}{k} \rceil$. Again using the formula $\lceil \frac{\lceil n/m \rceil}{k} \rceil = \lceil \frac{n}{mk} \rceil$ an upper bound for the total depth is given by

$$d(n) \leq 2(D + p) \times \left(\sum_{j=1}^{\lceil \log_2(n) \rceil} \lceil n/(k2^j) \rceil \right).$$

After calculation, we get

$$d(n) \leq \frac{2(D + p)}{k} n + 2(D + p)\lceil \log_2(n) \rceil. \tag{1}$$

Note that with $k = 1$ then $D = 0$, $p = 1$ and we recover the result of Theorem 3.2. We are now ready to prove our main result.

Corollary 3.2.2: The depth of the circuits given by the algorithm DaCSynth is upper bounded by $\frac{4}{3}n + 8\lceil \log_2(n) \rceil$ with n the number of qubits.

Proof: To improve our first result, we need to find more efficient syntheses of our blocks. We performed a brute-force search for square matrices of size $k = 1, 2, 3, 4, 5, 6$. The search consisted in a breadth-first search: starting from the partial permutations, row/columns operations were applied in a growing depth manner. We explore the set of binary matrices and compute the minimum depth required to reduce them to a partial permutation. In order to reduce the size of the search, we only considered matrices up to row and column permutations. For this purpose, we used standard techniques involving graph isomorphism to compute a canonical representative for each class [19]. The results are given in Table II. We recall that row and column operations can be performed in parallel. It is clear that for smaller rectangular

TABLE II Number of Binary Matrices Reachable for Different Number of Qubits and Circuit Depth (Up to Row/Column Permutations)

Depth \ Number of qubits	1	2	3	4	5	6
0	2	3	4	5	6	7
1		4	17	69	199	630
2			15	243	5052	194390
3					367	56583

cases the worst case depth cannot be larger. So by considering blocks of size 6 the depth in the worst case is $D = 3$ and $p = 1$. Replacing in (1) gives the result. ■

We want to insist on the fact that the current upper bound is to be improved. In fact any improvements in the zeroing of larger blocks can significantly improve the theoretical upper bound and its range validity given in Table I. For instance computing the worst case depth for $k = 7, 8, 9$, if possible, may lead to a better upper bound. Moreover, what happens if we stop the row and column operations once the maximum number of one-entries in each row and column is below an integer $p > 1$? If D decreases faster than p increases this would represent another improvement.

As we already mentioned, the synthesis algorithm proposed in [15] can in fact be seen as a special case where $A_1 = I$ and their strategy is also a block algorithm with blocks of size $\log_2(n)/2 \times \log_2(n)/2$ and $n/\log_2(n) \times \log_2(n)/2$. Yet, translated in our framework, they only use operations on columns and the flipping entries operation.

B. GREEDY ALGORITHM FOR STEPS 2 AND 3

In practice, we use a greedy algorithm to perform steps 2 and 3. We recall that we work on a matrix B that we want to zero with the following three available operations: 1) row operations; 2) column operations; and 3) flipping one entry. Note that row and column operations can be performed in parallel as this corresponds to CNOT circuits on two disjoint subsets of qubits.

At each step, we compute a sequence of row and column operations on B that minimizes the number of ones in B and that can be done in parallel. If we only consider row or column operations then the optimal sequence can be computed in a polynomial time. To do so, we create a directed graph $G_{\text{row}}/G_{\text{col}}$ whose nodes are the rows/columns of B and the edges $(i \to j)$ are weighted by the gain in the number of ones if we apply the row operation $i \to j$. The optimal sequence of row/column operations is given by the maximum weight matching in such graph, which can be computed in polynomial time using the Blossom algorithm [20].

However, when considering both row and column operations, things are not that simple. A row operation on B modifies G_{col} and a column operation modifies G_{row} so we cannot solve independently (or one after the other) the two problems in order to have an optimal sequence. The maximum weight matching problem on $G = (V, E)$ can be reformulated as a linear programming

$$\text{maximize} \sum_{e \in E} x_e w(e)$$

$$\text{such that} \sum_{e \in \{(u,v),(v,u) | v \in \delta(u)\}} x_e \leq 1 \text{for all vertices } u \in V$$

$$x_e \in \{0, 1\} \text{for all edges } e \in E \quad (2)$$

where $\delta(u)$ stands for the set of nodes adjacent to u. Taking into account both row and column operations adds quadratic terms in the cost function and that complicates the search for an optimal solution. Namely this new problem on the two graphs $G_{\text{row}} = (V_{\text{row}}, E_{\text{row}})$ and $G_{\text{col}} = (V_{\text{col}}, E_{\text{col}})$ can be reformulated as

$$\begin{aligned}\text{maximize} & \sum_{e_{\text{row}} \in E_{\text{row}}} x_{e_{\text{row}}} w(e_{\text{row}}) + \sum_{e_{\text{col}} \in E_{\text{col}}} x_{e_{\text{col}}} w(e_{\text{col}}) \\ & + \sum_{e_{\text{col}}, e_{\text{row}}} x_{e_{\text{row}}} x_{e_{\text{col}}} q(e_{\text{row}}, e_{\text{col}})\end{aligned}$$

$$\text{such that} \sum_{e_{\text{row}} \in \{(u,v),(v,u) | v \in \delta(u)\}} x_{e_{\text{row}}} \leq 1 \quad \text{for all vertices } u \in V_{\text{row}}$$

$$\sum_{e_{\text{col}} \in \{(u,v),(v,u) | v \in \delta(u)\}} x_{e_{\text{col}}} \leq 1 \quad \text{for all vertices } u \in V_{\text{col}}$$

$$x_e \in \{0, 1\} \quad \text{for all edges } e \in E_{\text{row}} \cup E_{\text{col}} \quad (3)$$

where the q's are the quadratic terms. Each quadratic term corresponds to a specific entry in B, so we have $q(e_{\text{row}}, e_{\text{col}}) \in \{-1, 0, 1\}$. Problem 3 is a particular instance of the *quadratic matching* problem where, given a graph G, one must find a matching that optimizes an objective function containing linear terms on the edges and quadratic terms on the pairs of edges. In Problem 3, the graph G is given by the disjoint union of the two graphs G_{row} and G_{col}, and the quadratic terms between two edges of G_{row} or two edges of G_{col} are 0. The quadratic matching problem is known to be NP-hard [21], is Problem 3 also NP-hard? We leave this question as a future work.

We still tried to solve exactly Problem 3 with an integer programming solver. Yet, given the quadratic terms the number of variables and constraints evolves as n^4 where n is the number of qubits and the method cannot find a solution even for $n = 10$. To get a nonoptimal solution in a reasonable amount of time, we compute a sequence of row and column operations greedily. We first choose the best row or column operation that minimizes the number of ones in B and we keep in memory the operation applied. Then, we determine the next best row or column operation among the operations that can be performed in parallel with the previously stored operation and we repeat the process. Finally if some rows and columns are left untouched we may complete the sequence

of operations by flipping some entries. The best sequence of flipping operations is computed as described in the proof of Theorem 3.2 using the Blossom algorithm. If no row or column operation can reduce the number of 1 in B then only the flipping operation is used.

IV. PURELY GREEDY ALGORITHMS

During steps 2 and 3 of the DaCSynth algorithm in Section III-B, we used a greedy process to zero a boolean matrix with as few operations as possible. We now explore the use of similar techniques directly on the linear boolean reversible operator to synthesize. It has been proven to be efficient for size optimization [22]. The method consists in a cost minimization technique. We need the following:

1) a cost function to minimize;
2) a strategy to explore the set of linear reversible operators.

Similarly to [22], we consider the following four cost functions to guide our search:

1) $h_{\text{sum}}(A) = \sum_{i,j} A_{i,j}$;
2) $H_{\text{sum}}(A) = h_{\text{sum}}(A) + h_{\text{sum}}(A^{-1})$;
3) $h_{\text{prod}}(A) = \sum_i \log_2(\sum_j A_{i,j})$;
4) $H_{\text{prod}}(A) = h_{\text{prod}}(A) + h_{\text{prod}}(A^{-1})$.

These four cost functions reach their minimum when A is a permutation matrix, motivating their use in a cost minimization process. If the cost function h_{sum} seems the first natural choice, the cost function h_{prod} has interesting features because it gives priority to "almost done" rows. Namely, if one row has only a few nonzero entries, the minimization process with h_{prod} will treat this row in priority and then it will not modify it anymore. This enables to avoid a problem, which one meets with the cost function h_{sum} where one ends up with a very sparse matrix but where the rows and columns have few nonzero common entries. This type of matrix represents a local minimum from which it can be difficult to escape. With this new cost function, as we put an additional priority on the rows with few remaining nonzero entries, we avoid this pitfall. Adding the cost of the inverse matrix also helps to escape from local minima.

In order to choose, which row and column operations to apply, we proceed similarly to the DaCSynth algorithm: we keep track of previously applied row and column operations to determine, which supplementary operations can be done without increasing the depth. At each iteration, we choose among the remaining operations that actually decrease the cost function the one that minimizes the cost function. If there are several possible operations, a random one is chosen. If no row or column operations can decrease the cost function, we reset simultaneously the set of row and column operations available. Every time the set of applied row or column operations is reset we increase a counter by one. The algorithm stops whether the current operator is a permutation matrix or when the counter exceeds a certain threshold.

We know from previous experiments [22] that such purely greedy algorithms behave extremely well on small operators (typically $n < 40$) or operators that need small/shallow circuits to be implemented. After a certain operator size or "complexity," the cost minimization process falls into local minima from which it is impossible to escape without a prohibitive overhead in the number of CNOTs or in the depth. One proposal to mitigate this behavior is to rely on an LU decomposition. It is well known that any operator A can be written

$$A = PLU$$

where P is a permutation matrix and L, U are triangular operators. We considered the case where we use our greedy algorithm on those triangular operators (the concatenation of the circuits obtained give a circuit for A up to the permutation P) with the hope that the expected bad scalability is mitigated at the price of worse results when the purely greedy methods perform well. Several triplets (P, L, U) are possible for one operator A. It was shown in [22] that it is possible to adopt specific strategies to compute (P, L, U). One of them consists in choosing iteratively the columns of L and rows of U to be the sparsest possible, this will be our approach and we will refer to this strategy as "LU sparse" in the benchmarks.

V. EXTENSION WITH ANCILLARY QUBITS

The quantum compiler Tpar efficiently reduces the T-depth by computing subsets of T gates that can be applied in parallel [10]. Each T gate is associated to a parity, i.e., a linear combination of the input qubits. With a subset of parities that are linearly independent, they can be computed at the same time and the T gates are applied in parallel to each qubit carrying one of these parities.

With ancillary qubits the parallelization can be even more efficient because the ancillary qubits can carry any parity, i.e., it can be a linear combination of the parities carried by nonancillary qubits. In terms of CNOT circuits synthesis, we need to synthesize a larger linear reversible operator. Namely we have to synthesize Boolean matrices of size $p \times n$ where $p - n$ is the number of additional qubits that will carry a parity. We extend our framework to treat this particular case. Our goal is, given an input operator $A_{\text{in}} \in F_2^{p\times n}$ and an output operator $A_{\text{out}} \in F_2^{p\times n}$, to synthesize an operator $B \in F_2^{p\times p}$ such that $BA_{\text{in}} = A_{\text{out}}$. The main difference with standard linear reversible circuit synthesis is that B is not unique so we need to find a suitable B and to synthesize it.

We propose a simple block algorithm and we prove that the total depth for the synthesis is equal, up to additive logarithmic terms, to the depth of the synthesis on an operator $A \in F_2^{p\times n}$, $n \leq p \leq 2n$. This result shows that the total depth barely increases with the number of ancillas after a certain threshold.

A BLOCK EXTENSION ALGORITHM

Let $A \in F_2^{p\times n}$. We assume that the first n rows of A form an invertible matrix. If not, we can always find a permutation

matrix P such that PA is as desired; see Section III. Given $p = kn + r$, we partition the operator A into k blocks of n rows and one block of r rows. As assumed the first block is of full rank and we merge it with the block of r rows.

The core of this extension algorithm lies in the idea that it is cheap to make each block invertible. Actually it can be done with a circuit of depth $\lceil \log_2(k) \rceil$ by using the following lemma.

Lemma 5.1: Given two matrices $A, B \in F_2^{n\times n}$ with A of full rank. There exists a partial permutation P such that $B + PA$ is of full rank.

Proof: Suppose B is of rank $k, k < n$. We can write $B = CD$ where $C \in F_2^{n\times k}$, $D \in F_2^{k\times n}$ are of rank k. One can always add a set of $n - k$ canonical vectors to the columns of C to create a basis of F_2^n. We can complete as well the rows of D into a basis of F_2^n by adding row vectors of A. We get two new extended matrices $C,' D'$ such that $B' = C'D'$ is now invertible. We can always add zero columns in C' and the remaining rows of A in D' and reorder the columns of C' and D' to get $C' = [C|P]$ and $D' = [D|A]$ with P a partial permutation matrix. Rewriting $B' = [C|D] \times [P|A] = CD + PA = B + PA$ proves the result. ■

To make all blocks invertible, we first make sure that the second block is of full rank by adding the appropriate rows of the first block. Using the lemma above this operation can be done with a circuit of depth 1. Then, we make sure that the third and fourth block are of full rank by adding the appropriate rows of the first and second block. Repeating this procedure, it is clear that we only need $\lceil \log_2(k) \rceil$ iterations to treat all the blocks.

What we want is an algorithm that synthesizes a circuit outputting an operator $A_{\text{out}} \in F_2^{p\times n}$ given an input operator $A_{\text{in}} \in F_2^{p\times n}$. Our proposal is to synthesize two operators B_1, B_2 such that the block partition of

$$B_1 A_{\text{in}} = \begin{pmatrix} K_1 \\ K_2 \\ \vdots \\ K_k \end{pmatrix}$$

and

$$B_2 A_{\text{out}} = \begin{pmatrix} H_1 \\ H_2 \\ \vdots \\ H_k \end{pmatrix}$$

contains only invertible blocks. Then, we can apply independently a linear reversible operator on each block to do the transition $B_1 A_{\text{in}} \to B_2 A_{\text{out}}$. Namely, for any $i > 1$, we apply $D_i = H_i K_i^{-1}$ to the ith block. For $i = 1$, we need an operator D_1 to do the transition $K_1 \to H_1 \in F_2^{(n+r)\times(n+r)}$. We did not particularly optimize this part, but as we know that the first n rows of K_1 form an invertible matrix, we consider an operator D_1 of the form

$$D_1 = \begin{pmatrix} H_1[1:n,:]K_1[1:n,:]^{-1} & 0 \\ G & I_{n-r} \end{pmatrix}$$

where each row of G contains the decomposition of each vector $K_1[i,:] \oplus H_1[i,:], i > n$ in the basis $K_1[1:n,:]$.

Overall we apply a block diagonal operator $D = \oplus_{i=1}^{k} D_i$ with $D_1 \in F_2^{(n+r)\times(n+r)}$ and $D_i \in F_2^{n\times n}$ for $i > 1$ such that

$$DB_1 A_{\text{in}} = B_2 A_{\text{out}}$$

and finally

$$A_{\text{out}} = B_2^{-1} D B_1 A_{\text{in}}.$$

The total depth of our circuit is the sum of the depth of the circuits implementing B_1, B_2, and D. We know that the depth for implementing B_1, B_2 does not exceed $\lceil \log_2(\lfloor p/n \rfloor) \rceil$ and most of the total depth lies in the synthesis of D. The synthesis of D requires a call to our framework for the square blocks of size n and one call for the first block of size $n + r$. All syntheses are performed simultaneously so the total depth for step 2 is given by the maximum depth required for the synthesis of one of the blocks.

The total depth $d(n, p)$ is given by

$$d(n, p) = 2\log_2(\lfloor p/n \rfloor) + d^*(n + r) \leq 4n + 2\log_2(\lfloor p/n \rfloor)$$

where $d^*(n + r)$ is the depth required to synthesize the block of size $(n + r) \times (n + r)$, which represents informally the maximum depth required when synthesizing all the blocks in parallel. The upper bound is not the tightest possible. The result we want to emphasize is that the depth only depends logarithmically on the number of ancillas.

VI. BENCHMARKS

This section presents our experimental results. We have the following algorithms to benchmark:

1) DaCSynth from Section III;
2) cost minimization techniques from Section IV;
3) the extension of DaCSynth for the use of ancillary qubits described in Section V.

The state-of-the-art algorithms are the following:

1) the Gaussian elimination algorithm;
2) the algorithm from [14] adapted to a full qubit connectivity, as described in Appendix A.

Two kinds of datasets are used to benchmark our algorithms.

1) First, a set of random operators. The test on random operators gives an overview of the average performance of the algorithms. We generate random operators by creating random CNOT circuits. Our routine takes two inputs: the number of qubit n and the depth d desired

for the random circuit. Each CNOT is randomly placed by selecting a random control and a random target and the simulation of the circuit gives a random operator. Empirically we noticed that when d is sufficiently large—$d = 2n$ is enough—then the operators generated have strong probability to represent the worst case scenarii. Alternatively, when only worst-case operators are of interest, it is faster to generate random circuits with a sufficiently large number of CNOT gates (n^2 gates is enough) instead of creating a circuit with a large depth.

2) Second, a set of reversible functions, given as circuits, taken from Matthew Amy's github repository [23]. This experiment shows how our algorithms (DaCSynth and the greedy procedures) can optimize useful quantum algorithms in the literature like the Galois Field multipliers, integer addition, Hamming coding functions, the hidden weighted bit functions, etc.

To evaluate the performance of our algorithms for the random set, two types of experiments are conducted as follows.

1) A worst-case asymptotic experiment, namely for increasing problem sizes n we generate circuits of depth $2n$ and we compute the average depth for each problem size. This experiment reveals the asymptotic behavior of the algorithms and gives insights about strict upper bounds on their performance.
2) A close-to-optimal experiment, namely for one specific problem size we generate operators with different circuit depth to show how close to optimal our algorithms are if the optimal circuits are expected to be shallower than the worst case.

To produce the benchmarks we need an explicit way to compute the depth. This task is less trivial than computing the number of gates in the circuits. The most common way to perform this computation is to create a directed acyclic graph representation of the circuit: the vertices of the graph are the gates and the edges represent their inputs/outputs. The depth of the circuit is then given by the longest path in the graph, which can be computed by doing a topological sorting of the vertices for example. Another way is to divide the circuit into slices of parallel gates. When a new gate is added to the circuit one has to pull it to its maximum to the left of the circuit by commuting it with the existing slices. If the gate cannot commute with the first slice it encounters, a new slice is created. The number of slices is then equal to the depth of the circuit. An interesting feature of this procedure is that we recover the skeleton circuit outlined in [17] by computing the depth on a circuit returned by a standard Gaussian elimination algorithm.

All our algorithms are implemented in Julia [24] and executed on the ATOS Quantum Learning Machine whose processor is an Intel Xeon E7-8890 v4 at 2.4 GHz.

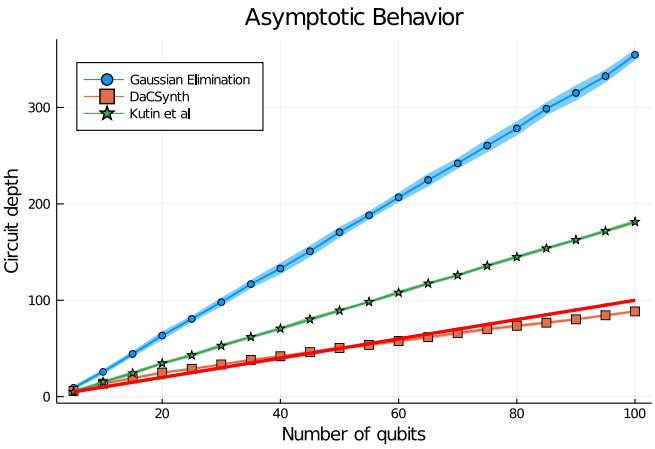

FIG. 1. Average performance of DaCSynth versus Gaussian elimination algorithm and [14].

A. BENCHMARKS ON RANDOM CIRCUITS

We did the following experiments:

1) We evaluated the worst case performance of the different algorithms for a range of qubits. For $n = 1, \ldots, 100$, we tested the algorithm on 20 random circuits with high depth $= 2n$ to reach with high probability the worst cases.
2) We also evaluated the capacity of the different algorithms to find shallow circuits for a specific problem size. For $n = 60$, we tested our algorithms on random circuits of various depth from 1 to ≈ 80 with 20 circuits for each depth.

1) EVALUATION OF DACSYNTH

For clarity we do not show all the methods at once. We first show the worst case performance of DaCSynth against the Gaussian elimination algorithm and Kutin *et al.*'s algorithm in Fig. 1. In this case, the three algorithms have a linear complexity, and we almost recover the theoretical worst case complexities: $\approx 4n$ for the Gaussian elimination algorithm, $\approx 2n$ for Kutin *et al*'s algorithm. The depth complexity of DaCSynth is close to n when $n < 50$ but tends to $0.85n$ when $n > 50$. For larger values of n not shown in this graph ($100 < n < 1000$) the depth complexity seems to remain around $0.85n$, so we cannot really say if this complexity actually hides a complexity in $n/\log_2(n)$ or not. Our current implementation cannot deal with larger number of qubits; it would be interesting to implement a more efficient version of DaCSynth to see how DaCSynth behaves and also to do a proper comparison with the algorithm from [15].

DaCSynth outperforms the state of the art by at least a factor of two, and this outperformance is also visible in the close-to-optimal experiment given in Fig. 2. DaCSynth still is able to resynthesize a circuit with small depth, although it cannot give optimal results. Overall, the behavior of those three algorithms (DaCSynth, the Gaussian Elimination, and the extension of Kutin *et al.*'s algorithm) is similar for any

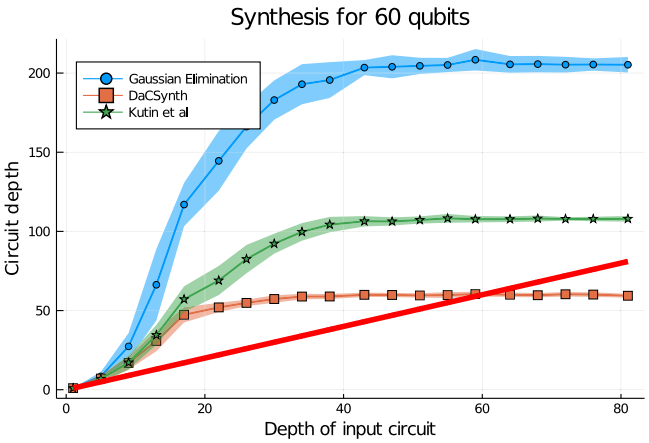

FIG. 2. Performance of DaCSynth versus Gaussian elimination algorithm and [14] on 60 qubits for different input circuits depths.

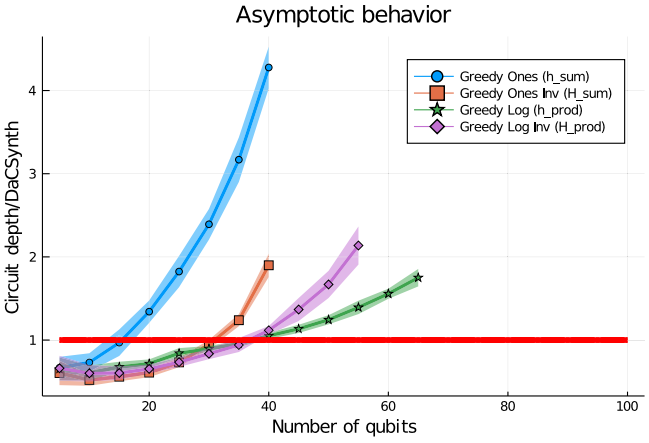

FIG. 3. Average performance of cost minimization techniques versus DaCSynth.

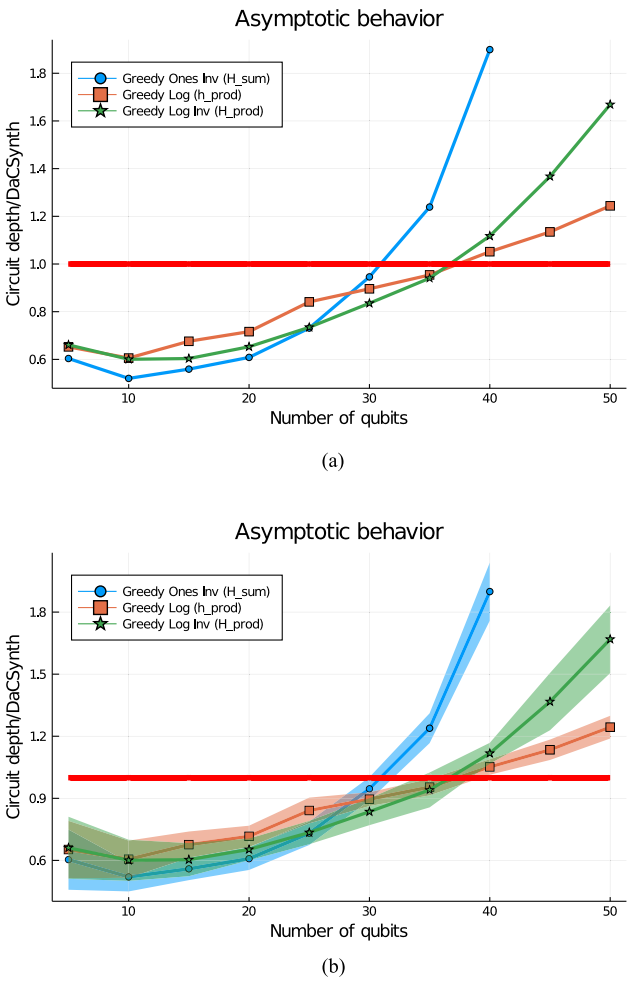

FIG. 4. Average performance of cost minimization techniques ($\{h_{\text{prod}}, H_{\text{sum}}, H_{\text{prod}}\}$) versus DaCSynth. (a) Average performance of cost minimization techniques($\{h_{\text{prod}}, H_{\text{sum}}, H_{\text{prod}}\}$) vs DaCSynth (without standard deviation). (b) Average performance of cost minimization techniques ($\{h_{\text{prod}}, H_{\text{sum}}, H_{\text{prod}}\}$) versus DaCSynth (with standard deviation).

problem size. Consequently for the rest of the benchmarks, we now consider DaCSynth as the state-of-the-art method.

2) EVALUATION OF THE PURELY GREEDY ALGORITHMS

We now evaluate the performance of our greedy algorithms against DaCSynth. The results of the worst-case experiment are given in Figs. 3 and 4. For clarity we plot the ratio between the depth of the circuits returned by the greedy algorithms and the depth of the circuits returned by DaCSynth. So when the ratio is smaller than one this means that the greedy method outperforms DaCSynth. The results with the four cost functions are given in Fig. 3. For small n the greedy methods always outperform DaCSynth; but inevitably as n grows the performance of the greedy methods deteriorates, and this occurs exponentially fast. In fact, when n is sufficiently large the cost minimization process can no longer converge to a solution, and we stop the experiments when it is clear that the cost minimization process cannot outperform DaCSynth. The bad scalability of the greedy methods is particularly visible with the cost function h_{sum}. Clearly this cost function is always outperformed by the three others, but the scale of the figure prevents proper discernment of the performance of the other three cost functions. A zoom in the range $n = 0.50$ without the cost function h_{sum} is proposed in Fig. 4. In a way, we get results similar to those obtained for a size optimization approach in [22]. The H_{sum} cost function provides the best results for $n < 25$ but its performances deteriorate faster than with the log based cost functions. However, contrary to the size optimization case where we highlighted a slight range of qubits where the cost function h_{prod} could perform better than H_{sum}, here this is the cost function H_{prod} that seems to give the best results for the approximate range $n = 25.40$. However, when we plot the results with the standard deviation in Fig. 4(b), we see that this advantage of one cost function over the others is relative in view of the high variance in the results. We recover similar results with the close-to-optimal experiment, see Fig. 5. The two cost functions H_{sum} and H_{prod} provides what seems to be optimal results when the input operator is generated with

IEEE Transactions on Quantum Engineering

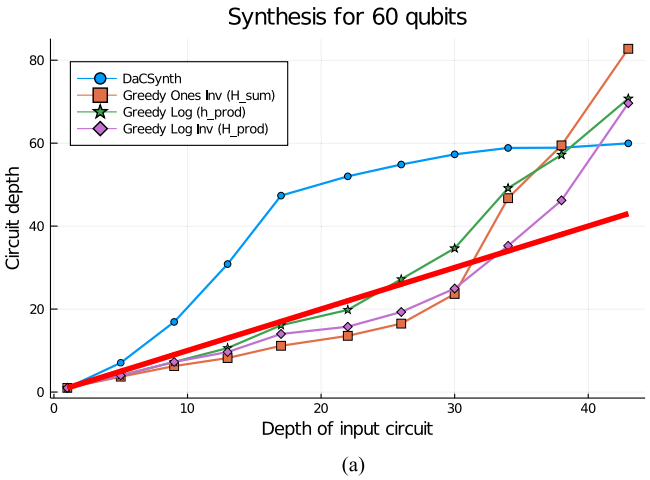

(a)

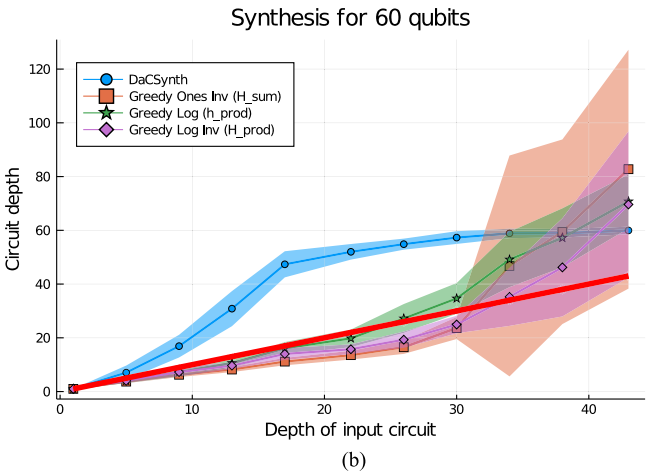

(b)

FIG. 5. Performance of cost minimization techniques ($\{h_{\text{prod}}, H_{\text{sum}}, H_{\text{prod}}\}$) and DaCSynth on 60 qubits. (a) Performance of cost minimization techniques ($\{h_{\text{prod}}, H_{\text{sum}}, H_{\text{prod}}\}$) and DaCSynth on 60 qubits for different input circuits depths (without standard deviation). (b) Performance of cost minimization techniques ($\{h_{\text{prod}}, H_{\text{sum}}, H_{\text{prod}}\}$) versus DaCSynth on 60 qubits for different input circuits depths (with standard deviation).

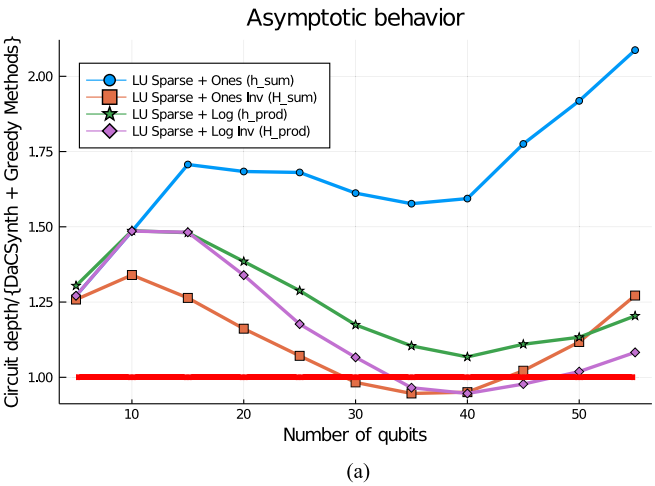

(a)

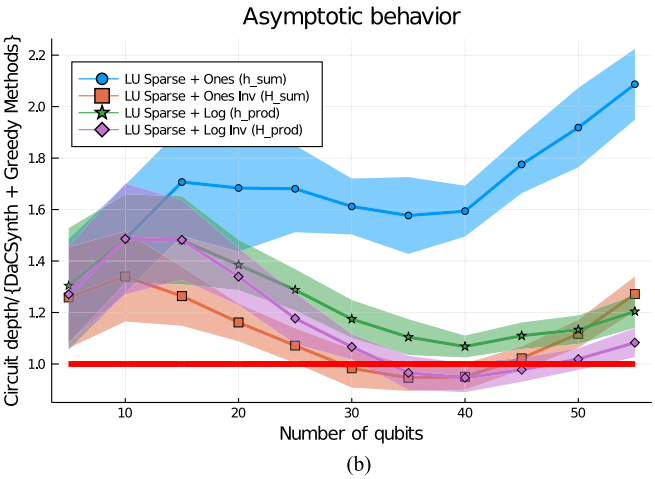

(b)

FIG. 6. Average performance of { LU decomposition + greedy methods } versus { DaCSynth and purely greedy methods }. (a) Average performance of { LU decomposition + greedy methods } versus { DaCSynth and purely greedy methods } (without standard deviation). (b) Average performance of { LU decomposition + greedy methods } versus { DaCSynth and purely greedy methods } (with standard deviation).

a shallow circuit. In fact both cost functions consistently enable to resynthesize the operator with a shallower circuit than the one given as input. There is a threshold when the input circuits are of depth 30 or larger and it becomes harder for the cost minimization technique to converge promptly to a solution. The performance of our greedy methods deteriorate with a high variance in the results, especially with the H_{sum} cost function; see Fig. 5(b). Finally, when we get closer and closer to a worst case DaCSynth eventually provides the best results, in accordance with the worst case experiment done previously.

We also did some experiments with the greedy algorithms combined with the LU decomposition. We only show the worst-case experiment results in Fig. 6. The ratio between the method benchmarked and the best result among the purely greedy methods and DaCSynth is plotted. So if the value of the curve is below one this means that the algorithm outperforms all the other ones we have studied so far. Overall there is a range of qubits (between 30 and 45) where the association of the LU decomposition and the greedy methods slightly provides the best results. Again this advantage must be nuanced because the variance of the results is quite high [see Fig. 6(b)]. Less significant results were obtained in the close-to-optimal experiment so we do not report them.

Overall, for practical synthesis problems, e.g., for the library of reversible functions we consider in Section VI-B, it is preferable to try all three cost functions, with and without the LU decomposition, and keep the best result. Globally all the execution times required for the greedy methods are in the same range of magnitude, so we only increase the total execution time by a factor given by the number of methods we want to try. Further analysis needs to be done to determine when each method should be used.

B. BENCHMARKS ON REVERSIBLE FUNCTIONS

We apply our method to the synthesis of well-known reversible functions. Our goal is to show that we can mitigate the CNOT cost of the circuits while keeping the T-cost as low as possible. Our strategy is simple: we scan a circuit where the T-cost has been optimized and we resynthesize each CNOT subcircuit appearing. This way we keep the T-count and the T-depth as low as possible. We already showed in [22] that the CNOT count can be significantly reduced, but also the depth to our surprise. Here, we focus primarily on depth optimization.

We choose the Tpar algorithm [10] for the preprocessing part: this is the best algorithm to our knowledge for the T-depth optimization. The Tpar algorithm also works with ancillary qubits and requires the synthesis of linear reversible circuits with encoded ancillas, where we can use the extension of our framework. Since Tpar, other algorithms optimizing the T-count have been proposed [6]–[9] and can be plugged before the Tpar algorithm in the preprocessing part. Even though such algorithms provide better T-counts, the T-par algorithm alone remains competitive for the T-count and we believe using only Tpar does not alter the global message of this section, which is that the depth of reversible circuits can be significantly reduced without increasing other metrics of importance like the T-depth. So, for simplicity, we do not consider those newer T-count optimizers.

The library of reversible functions we used is taken from Matthew Amy's github repository [23]. Still from Matthew Amy's github repository we used his C++ implementation of the Tpar algorithm. Although a more recent implementation in Haskell exists, by the time we write this article it does not take into account ancillary qubits.

1) ANCILLA-FREE RESULTS

Without ancillary qubits, the results are given in Table III. For each reversible function, we provide the statistics (T-count, T-depth, CNOT count, Total depth) of the original circuit and the circuit optimized solely with the Tpar algorithm. As the T-count and T-depth remain unchanged after our postoptimization process, we only show the new CNOT count and total depth after running our framework for size optimization from [22] and our framework for depth optimization described in this article. For those two metrics (CNOT count and total depth) the savings compared to the Tpar algorithm are also given.

We also compare ourselves against a heuristic optimization from Nam, Ross, Su, Childs, and Maslov [25], which is now one of the state-of-the-art methods for quantum circuits optimization. Although its primary objective is gate count optimization, the heuristic also improves the total depth of the circuits. Two versions of their algorithm are proposed, corresponding to "light" and "heavy" optimization procedures. The code is not open source, but the circuits are available in Neil Ross's github repository [26]. So, when available, we chose the results of the heavy optimization and reported them in Table III.

Compared to Tpar, for almost every function we manage to reduce significantly the total depth: -47% in average, with a maximum of -92%. The Galois field multipliers are notably the functions that benefit the most from our optimization with at least 65% of reduction. As a bonus, we also have better CNOT counts with 40% of gain in average.

The heuristic from [25] gives the best CNOT counts of the four methods by far. This significant decrease in the CNOT count has also a beneficial impact on the total depth but these gains come at the expense of another metric of importance: the T-depth. More exactly, the heuristic does not benefit from the optimizations done by Tpar, which results in a difference in the T-depth of more than 100% in almost every circuit, with up to 760% for the GF(2^{32}) multiplier. Still, we manage to produce circuits with equivalent or even better depths than [25] for 70% of the circuits. Again, our best gains are for the Galois field multipliers with 35%–40% in average except for GF(2^{32}) with a gain of 12%. There are five circuits for which our method gives significant worse results with an increase of more than 10% in the depth.

Compared to the size optimization framework proposed in [22], we manage to produce better results for almost every function—the only exception being the Barenco version of the Toffoli gate on 3 qubits. Again the Galois field multipliers are significantly optimized: for the multiplier in GF(2^{32}), we reduced the depth from 2130 to 888, representing a relative gain of 58%. Yet this comes at the price of an increased CNOT count.

Overall, these results show that it is possible to significantly optimize the depths of useful circuits while keeping other metrics of importance like the T-depth optimized. We improve a precedent framework that achieves a similar goal but with a focus on size optimization. Compared to a state-of-the-art method that does not optimize the T-depth, we also manage to provide circuits of similar or even better depths, proving that the optimization of the T-depth and the total depth are not incompatible. As future work, it would be interesting to design an algorithm that solely focuses on total depth optimization (without particular consideration on the T-depth) and see how our framework compares against.

To evaluate which algorithm was actually useful for providing the best results, we also give in Table IV the frequency of best performance for each algorithm. More precisely for each method, we give the number of times it returned the best result and the number of times it was the only method to return the best result. In [22], we observed that the greedy methods for optimizing the size gave most of the times the best results, emphasizing the idea that overall most of the subcircuits to resynthesize correspond to simple operators. We observe a similar pattern here: we could have done the same experiment with solely the greedy algorithms with the three cost functions H_{sum}, h_{prod}, and H_{prod}. Even though most of the time they all provide the best results, for some specific

TABLE III CNOT Optimization of a Library of Reversible Functions With Several CNOT Circuits Synthesis Methods. For Each Reversible Function, "original" Reports Some Statistics (T-Count, T-Depth, CNOT Count, Total Depth) of the Original Circuit, "tpar" Reports the Results of the Circuit Optimized Solely by the Tpar Algorithm, "tpar + CNOT Size Opt." Reports the Results of the Circuit Optimized With the Tpar Algorithm and Postprocessed by a Size Optimization Procedure from [22] and Finally "tpar + CNOT Depth Opt." Reports the Results of the Circuit Optimized With the Tpar Algorithm and Post-Processed by Our Proposed Depth Optimization Procedure. The T-Count and T-Depth for the Last Two Algorithms are Omitted Because Identical to the Tpar Algorithm

Function	#n	Original				Tpar [10]				Nam *et al.* [25]							Tpar + CNOT size opt. [22]				Tpar + CNOT depth opt.				
		T-count	T-depth	CNOT count	Depth	T-count	T-depth	CNOT count	Depth	T-count	T-depth	%Diff. (vs T-par)	CNOT count	%Diff. (vs T-par)	Depth	%Diff. (vs T-par)	CNOT count	%Diff. (vs T-par)	Depth	% Diff. (vs T-par)	CNOT count	%Diff. (vs T-par)	Depth	% Diff. (vs T-par)	% Diff. (vs Nam *et al.*)
Adder_8	24	399	69	466	223	213	30	741	302	215	73	+143%	291	−61%	193	−36%	491	−34%	200	−34%	511	−31%	190	−37%	−2%
barenco_tof_10	19	224	96	224	288	100	43	332	272	100	81	+88%	130	−61%	230	−15%	188	−43%	217	−20%	188	−43%	215	−21%	−7%
barenco_tof_3	5	28	12	28	36	16	8	52	60	16	16	+100%	18	−65%	38	−37%	26	−50%	34	−43%	26	−50%	35	−42%	−8%
barenco_tof_4	7	56	24	56	72	28	13	96	96	28	27	+108%	34	−65%	68	−29%	50	−48%	61	−36%	50	−48%	61	−36%	−10%
barenco_tof_5	9	84	36	84	108	40	18	134	123	40	36	+100%	50	−63%	95	−23%	73	−46%	89	−28%	73	−46%	87	−29%	−8%
csla_mux_3	15	70	21	90	67	62	8	379	210	64	26	+225%	70	−82%	63	−70%	187	−51%	85	−60%	195	−49%	69	−67%	+10%
csum_mux_9	30	196	18	196	59	84	6	366	153	84	16	+167%	140	−62%	47	−69%	179	−51%	76	−50%	194	−47%	59	−61%	+26%
cycle_17_3	35	4739	2001	4742	5974	1944	562	6608	5231	-	-	-	-	-	-	-	4267	−35%	4215	−19%	4810	−27%	3884	−26%	-
GF(2^{10})_mult	30	700	108	709	290	410	16	2206	1026	410	117	+631%	609	−72%	291	−72%	949	−57%	299	−71%	1124	−49%	192	−81%	−34%
GF(2^{16})_mult	48	1792	180	1837	489	1040	24	6724	2551	1040	196	+717%	1581	−76%	492	−81%	2545	−62%	687	−73%	3314	−51%	345	−86%	−30%
GF(2^{32})_mult	96	7168	372	7292	1001	4128	47	34244	11520	4128	404	+760%	6299	−82%	1006	−91%	10972	−68%	2130	−82%	15680	−54%	888	−92%	−12%
GF(2^{4})_mult	12	112	36	115	99	68	6	307	173	68	40	+567%	99	−68%	102	−41%	135	−56%	77	−55%	154	−50%	61	−65%	−40%
GF(2^{5})_mult	15	175	48	179	130	115	9	502	259	115	53	+489%	154	−69%	131	−49%	210	−58%	117	−55%	236	−53%	80	−69%	−39%
GF(2^{6})_mult	18	252	60	257	163	150	9	660	350	150	66	+633%	221	−67%	166	−53%	308	−53%	134	−62%	372	−44%	95	−73%	−43%
GF(2^{7})_mult	21	343	72	349	195	217	12	996	490	217	80	+567%	300	−70%	198	−60%	442	−56%	178	−64%	524	−47%	127	−74%	−36%
GF(2^{8})_mult	24	448	84	469	233	264	13	1254	619	264	92	+608%	405	−68%	236	−62%	589	−53%	223	−64%	691	−45%	146	−76%	−38%
GF(2^{9})_mult	27	567	96	575	258	351	15	1712	810	351	105	+600%	494	−71%	259	−68%	753	−56%	272	−66%	894	−48%	160	−80%	−38%
grover_5	9	336	144	336	457	154	51	499	477	-	-	-	-	-	-	-	331	−34%	377	−21%	332	−33%	370	−22%	-
ham15-high	20	2457	996	2500	3026	1019	380	3427	2956	-	-	-	-	-	-	-	2183	−36%	2227	−25%	2261	−34%	2153	−27%	-
ham15-low	17	161	69	259	263	97	33	471	360	-	-	-	-	-	-	-	280	−41%	221	−39%	294	−38%	206	−43%	-
ham15-med	17	574	240	616	750	230	84	759	682	-	-	-	-	-	-	-	481	−37%	503	−26%	492	−35%	490	−28%	-
hwb6	7	105	45	131	152	75	24	270	248	-	-	-	-	-	-	-	172	−36%	157	−37%	177	−34%	153	−38%	-
hwb8	12	5887	2139	7970	7956	3531	860	22670	15838	-	-	-	-	-	-	-	13351	−41%	9120	−42%	14226	−37%	8247	−48%	-
mod5_4	5	28	12	32	41	16	6	48	57	16	14	+133%	28	−42%	46	−19%	32	−33%	39	−32%	33	−31%	40	−30%	−13%
mod_adder_1024	28	1995	831	2005	2503	1011	258	3650	2560	1011	743	+188%	1278	−65%	2086	−19%	2369	−35%	1906	−26%	2575	−29%	1755	−31%	−16%
mod_adder_1048576	58	17290	7292	17310	21807	7298	1927	29794	19975	-	-	-	-	-	-	-	19122	−36%	15258	−24%	21179	−29%	14055	−30%	
mod_mult_55	9	49	15	55	50	35	7	106	75	35	19	+171%	40	−62%	47	−37%	73	−31%	52	−31%	75	−29%	50	−33%	+6%
mod_red_21	11	119	48	122	158	73	25	223	207	73	50	+100%	77	−65%	129	−38%	136	−39%	145	−30%	139	−38%	137	−34%	+6%
qcla_adder_10	36	238	24	267	73	162	13	648	195	162	26	+100%	183	−72%	63	−68%	363	−44%	92	−53%	375	−42%	85	−56%	+35%
qcla_com_7	24	203	27	215	81	94	12	371	154	95	26	+117%	132	−64%	69	−55%	202	−46%	82	−47%	208	−44%	77	−50%	+12%
qcla_mod_7	26	413	66	441	197	231	28	813	296	235	72	+157%	292	−64%	183	−38%	479	−41%	176	-41%	494	−39%	169	−43%	−8%
qft_4	5	69	48	48	142	67	44	96	185	-	-	-	-	-	-	-	56	−42%	150	−19%	56	−42%	149	−19%	-
rc_adder_6	14	77	33	104	104	47	22	165	157	47	31	+41%	71	−57%	83	−47%	100	−39%	103	−34%	100	−39%	95	−39%	+14%
tof_10	19	119	51	119	153	71	27	236	190	71	55	+104%	70	−70%	136	−28%	130	−45%	140	-26%	132	−44%	136	−28%	0%
tof_3	5	21	9	21	27	15	6	35	46	15	13	+117%	14	−60%	31	−33%	21	−40%	31	−33%	21	−40%	31	−33%	0%
tof_4	7	35	15	35	45	23	9	63	71	23	19	+111%	22	−65%	46	−35%	37	−41%	49	−31%	39	−38%	43	−39%	−7%
tof_5	9	49	21	49	63	31	12	97	104	31	25	+108%	30	−69%	61	−41%	50	−48%	67	−36%	52	−46%	63	−39%	+3%
vbe_adder_3	10	70	24	80	79	24	9	120	88	24	16	+78%	50	−58%	56	−36%	61	−49%	46	−48%	61	−49%	45	−49%	−20%
Mean difference												+276.8%		−66%		−46.55%		−45.03%		−41.66%		−41.37%		−46.68%	−10.24%
Worst savings												+760%		−42%		−15%		−31%		-19%		−27%		−19%	+35%
Best savings												+41%		−82%		−91%		−68%		-82%		−54%		−92%	−43%

TABLE IV Frequency of Best Performance of Each Algorithm During the Optimization of Reversible Circuits. For Each Algorithm, the First Column Gives the Number of Times It Has Returned the Best Result (Possibly Other Algorithms Returned Circuits of Same Size). The Second Column Reports the Number of Times It Was the Only One to Provide the Best Possible Circuit

Function	#n	#CNOT sub-circuits	Kutin et al		DaCSynth		Greedy (H_{sum}, size)		Greedy (h_{prod}, size)		Greedy (H_{sum})		Greedy (h_{prod})		Greedy (H_{prod})		LU + Greedy (H_{sum})		LU + Greedy (H_{prod})	
			Best choice	Only Choice	Best choice	Only Choice	Best choice	Only Choice	Best choice	Only Choice	Best choice	Only Choice	Best choice	Only Choice	Best choice	Only Choice	Best choice	Only Choice	Best choice	Only Choice
Adder_8	24	60	29 (48%)	0 (0%)	15 (25%)	0 (0%)	39 (65%)	0 (0%)	38 (63%)	0 (0%)	60 (100%)	3 (5%)	53 (88%)	0 (0%)	53 (88%)	0 (0%)	37 (62%)	0 (0%)	38 (63%)	0 (0%)
barenco_tof_10	19	99	64 (65%)	0 (0%)	44 (44%)	0 (0%)	99 (100%)	0 (0%)	99 (100%)	0 (0%)	99 (100%)	0 (0%)	99 (100%)	0 (0%)	99 (100%)	0 (0%)	83 (84%)	0 (0%)	83 (84%)	0 (0%)
barenco_tof_3	5	14	11 (79%)	0 (0%)	7 (50%)	0 (0%)	14 (100%)	0 (0%)	14 (100%)	0 (0%)	14 (100%)	0 (0%)	14 (100%)	0 (0%)	14 (100%)	0 (0%)	12 (86%)	0 (0%)	12 (86%)	0 (0%)
barenco_tof_4	7	27	20 (74%)	0 (0%)	15 (56%)	0 (0%)	27 (100%)	0 (0%)	27 (100%)	0 (0%)	27 (100%)	0 (0%)	27 (100%)	0 (0%)	27 (100%)	0 (0%)	24 (89%)	0 (0%)	24 (89%)	0 (0%)
barenco_tof_5	9	39	27 (69%)	0 (0%)	20 (51%)	0 (0%)	39 (100%)	0 (0%)	39 (100%)	0 (0%)	39 (100%)	0 (0%)	39 (100%)	0 (0%)	39 (100%)	0 (0%)	32 (82%)	0 (0%)	32 (82%)	0 (0%)
csla_mux_3	15	15	1 (7%)	0 (0%)	1 (7%)	0 (0%)	6 (40%)	0 (0%)	2 (13%)	0 (0%)	13 (87%)	1 (7%)	12 (80%)	2 (13%)	12 (80%)	0 (0%)	5 (33%)	0 (0%)	5 (33%)	0 (0%)
csum_mux_9	30	14	5 (36%)	0 (0%)	2 (14%)	0 (0%)	5 (36%)	0 (0%)	5 (36%)	0 (0%)	12 (86%)	4 (29%)	9 (64%)	2 (14%)	7 (50%)	0 (0%)	5 (36%)	0 (0%)	5 (36%)	0 (0%)
cycle_17_3	35	1436	725 (50%)	0 (0%)	433 (30%)	0 (0%)	871 (61%)	0 (0%)	840 (58%)	0 (0%)	1417 (99%)	4 (0%)	1211 (84%)	12 (1%)	1385 (96%)	1 (0%)	910 (63%)	0 (0%)	913 (64%)	0 (0%)
GF(2^{10})_mult	30	20	1 (5%)	0 (0%)	1 (5%)	0 (0%)	2 (10%)	0 (0%)	2 (10%)	0 (0%)	16 (80%)	6 (30%)	8 (40%)	1 (5%)	11 (55%)	2 (10%)	1 (5%)	0 (0%)	1 (5%)	0 (0%)
GF(2^{16})_mult	48	28	1 (4%)	0 (0%)	1 (4%)	0 (0%)	1 (4%)	0 (0%)	1 (4%)	0 (0%)	17 (61%)	6 (21%)	6 (21%)	3 (11%)	18 (64%)	7 (25%)	1 (4%)	0 (0%)	1 (4%)	0 (0%)
GF(2^{32})_mult	96	51	1 (2%)	0 (0%)	1 (2%)	0 (0%)	1 (2%)	0 (0%)	1 (2%)	0 (0%)	13 (25%)	5 (10%)	10 (20%)	6 (12%)	40 (78%)	30 (59%)	1 (2%)	0 (0%)	1 (2%)	0 (0%)
GF(2^{4})_mult	12	10	2 (20%)	0 (0%)	1 (10%)	0 (0%)	3 (30%)	0 (0%)	2 (20%)	0 (0%)	8 (80%)	1 (10%)	7 (70%)	1 (10%)	8 (80%)	0 (0%)	2 (20%)	0 (0%)	2 (20%)	0 (0%)
GF(2^{5})_mult	15	13	1 (8%)	0 (0%)	2 (15%)	0 (0%)	3 (23%)	0 (0%)	2 (15%)	0 (0%)	12 (92%)	4 (31%)	5 (38%)	0 (0%)	8 (62%)	1 (8%)	3 (23%)	0 (0%)	3 (23%)	0 (0%)
GF(2^{6})_mult	18	13	2 (15%)	0 (0%)	2 (15%)	0 (0%)	1 (8%)	0 (0%)	1 (8%)	0 (0%)	10 (77%)	5 (38%)	6 (46%)	0 (0%)	8 (62%)	1 (8%)	2 (15%)	0 (0%)	2 (15%)	0 (0%)
GF(2^{7})_mult	21	16	4 (25%)	0 (0%)	1 (6%)	0 (0%)	1 (6%)	0 (0%)	1 (6%)	0 (0%)	14 (88%)	5 (31%)	6 (38%)	0 (0%)	10 (62%)	1 (6%)	4 (25%)	0 (0%)	4 (25%)	0 (0%)
GF(2^{8})_mult	24	17	2 (12%)	0 (0%)	1 (6%)	0 (0%)	2 (12%)	0 (0%)	2 (12%)	0 (0%)	16 (94%)	9 (53%)	7 (41%)	0 (0%)	7 (41%)	0 (0%)	2 (12%)	0 (0%)	2 (12%)	0 (0%)
GF(2^{9})_mult	27	19	2 (11%)	0 (0%)	1 (5%)	0 (0%)	3 (16%)	0 (0%)	3 (16%)	0 (0%)	15 (79%)	6 (32%)	8 (42%)	2 (11%)	9 (47%)	2 (11%)	4 (21%)	0 (0%)	3 (16%)	0 (0%)
grover_5	9	123	85 (69%)	0 (0%)	55 (45%)	0 (0%)	113 (92%)	0 (0%)	111 (90%)	0 (0%)	123 (100%)	0 (0%)	122 (99%)	0 (0%)	122 (99%)	0 (0%)	102 (83%)	0 (0%)	101 (82%)	0 (0%)
ham15-high	20	852	527 (62%)	0 (0%)	343 (40%)	0 (0%)	746 (88%)	0 (0%)	727 (85%)	0 (0%)	845 (99%)	5 (1%)	831 (98%)	4 (0%)	833 (98%)	1 (0%)	653 (77%)	0 (0%)	657 (77%)	0 (0%)
ham15-low	17	69	43 (62%)	0 (0%)	30 (43%)	0 (0%)	50 (72%)	0 (0%)	49 (71%)	0 (0%)	64 (93%)	1 (1%)	67 (97%)	3 (4%)	61 (88%)	0 (0%)	47 (68%)	0 (0%)	47 (68%)	0 (0%)
ham15-med	17	189	135 (71%)	0 (0%)	84 (44%)	0 (0%)	173 (92%)	0 (0%)	168 (89%)	0 (0%)	187 (99%)	1 (1%)	187 (99%)	1 (1%)	186 (98%)	0 (0%)	163 (86%)	0 (0%)	165 (87%)	0 (0%)
hwb6	7	48	29 (60%)	0 (0%)	16 (33%)	0 (0%)	36 (75%)	0 (0%)	31 (65%)	0 (0%)	48 (100%)	1 (2%)	45 (94%)	0 (0%)	44 (92%)	0 (0%)	34 (71%)	0 (0%)	31 (65%)	0 (0%)
hwb8	12	2130	523 (25%)	0 (0%)	368 (17%)	1 (0%)	1084 (51%)	2 (0%)	913 (43%)	1 (0%)	2048 (96%)	109 (5%)	1835 (86%)	44 (2%)	1792 (84%)	4 (0%)	1005 (47%)	2 (0%)	961 (45%)	0 (0%)
mod5_4	5	14	9 (64%)	0 (0%)	10 (71%)	0 (0%)	13 (93%)	0 (0%)	14 (100%)	0 (0%)	14 (100%)	0 (0%)	14 (100%)	0 (0%)	13 (93%)	0 (0%)	14 (100%)	0 (0%)	14 (100%)	0 (0%)
mod_adder_1024	28	716	372 (52%)	0 (0%)	243 (34%)	0 (0%)	482 (67%)	0 (0%)	469 (66%)	0 (0%)	693 (97%)	0 (0%)	664 (93%)	4 (1%)	662 (92%)	1 (0%)	511 (71%)	0 (0%)	507 (71%)	0 (0%)
mod_adder_1048576	58	5615	2695 (48%)	0 (0%)	1581 (28%)	0 (0%)	3527 (63%)	0 (0%)	3444 (61%)	0 (0%)	5450 (97%)	13 (0%)	4926 (88%)	74 (1%)	5137 (91%)	0 (0%)	3635 (65%)	0 (0%)	3610 (64%)	0 (0%)
mod_mult_55	9	14	6 (43%)	0 (0%)	5 (36%)	0 (0%)	7 (50%)	0 (0%)	6 (43%)	0 (0%)	13 (93%)	0 (0%)	11 (79%)	0 (0%)	13 (93%)	1 (7%)	6 (43%)	0 (0%)	6 (43%)	0 (0%)
mod_red_21	11	46	31 (67%)	0 (0%)	19 (41%)	0 (0%)	39 (85%)	0 (0%)	36 (78%)	0 (0%)	46 (100%)	0 (0%)	43 (93%)	0 (0%)	44 (96%)	0 (0%)	38 (83%)	0 (0%)	38 (83%)	0 (0%)
qcla_adder_10	36	24	10 (42%)	0 (0%)	4 (17%)	0 (0%)	15 (62%)	0 (0%)	10 (42%)	0 (0%)	23 (96%)	1 (4%)	19 (79%)	0 (0%)	23 (96%)	0 (0%)	18 (75%)	0 (0%)	16 (67%)	0 (0%)
qcla_com_7	24	26	10 (38%)	0 (0%)	5 (19%)	0 (0%)	18 (69%)	0 (0%)	19 (73%)	0 (0%)	25 (96%)	1 (4%)	24 (92%)	1 (4%)	23 (88%)	0 (0%)	14 (54%)	0 (0%)	13 (50%)	0 (0%)
qcla_mod_7	26	52	19 (37%)	0 (0%)	8 (15%)	0 (0%)	38 (73%)	0 (0%)	37 (71%)	0 (0%)	51 (98%)	1 (2%)	45 (87%)	0 (0%)	49 (94%)	1 (2%)	33 (63%)	0 (0%)	30 (58%)	0 (0%)
qft_4	5	29	24 (83%)	0 (0%)	17 (59%)	0 (0%)	29 (100%)	0 (0%)	29 (100%)	0 (0%)	29 (100%)	0 (0%)	29 (100%)	0 (0%)	29 (100%)	0 (0%)	28 (97%)	0 (0%)	28 (97%)	0 (0%)
rc_adder_6	14	49	41 (84%)	0 (0%)	29 (59%)	0 (0%)	49 (100%)	0 (0%)	49 (100%)	0 (0%)	49 (100%)	0 (0%)	49 (100%)	0 (0%)	49 (100%)	0 (0%)	43 (88%)	0 (0%)	43 (88%)	0 (0%)
tof_10	19	52	41 (79%)	0 (0%)	22 (42%)	0 (0%)	42 (81%)	0 (0%)	41 (79%)	0 (0%)	52 (100%)	0 (0%)	51 (98%)	0 (0%)	51 (98%)	0 (0%)	45 (87%)	0 (0%)	47 (90%)	0 (0%)
tof_3	5	12	11 (92%)	0 (0%)	8 (67%)	0 (0%)	12 (100%)	0 (0%)	12 (100%)	0 (0%)	12 (100%)	0 (0%)	12 (100%)	0 (0%)	12 (100%)	0 (0%)	11 (92%)	0 (0%)	11 (92%)	0 (0%)
tof_4	7	17	15 (88%)	0 (0%)	10 (59%)	0 (0%)	15 (88%)	0 (0%)	15 (88%)	0 (0%)	17 (100%)	0 (0%)	16 (94%)	0 (0%)	16 (94%)	0 (0%)	16 (94%)	0 (0%)	16 (94%)	0 (0%)
tof_5	9	22	17 (77%)	0 (0%)	11 (50%)	0 (0%)	19 (86%)	0 (0%)	19 (86%)	0 (0%)	22 (100%)	0 (0%)	21 (95%)	0 (0%)	22 (100%)	0 (0%)	18 (82%)	0 (0%)	18 (82%)	0 (0%)
vbe_adder_3	10	19	12 (63%)	0 (0%)	9 (47%)	0 (0%)	18 (95%)	0 (0%)	16 (84%)	0 (0%)	19 (100%)	0 (0%)	19 (100%)	0 (0%)	19 (100%)	0 (0%)	18 (95%)	0 (0%)	15 (79%)	0 (0%)

TABLE V CNOT Optimization of a Library of Reversible Functions With Several CNOT Circuits Synthesis Methods With the Use of Ancillary Qubits. For Each Reversible Function, "original" Reports Some Statistics (T-Count, T-Depth, CNOT Count, Total Depth) of the Original Circuit, "tpar" Reports the Results of the Circuit Optimized Solely by the Tpar Algorithm, "tpar + CNOT Depth Opt." Reports the Results of the Circuit Optimized With the Tpar Algorithm and Postprocessed by Our Proposed Depth Optimization Procedure

Function	#n	#Ancillae	Original				Tpar (∞ ancillae)				Tpar + CNOT depth opt.			
			T-count	T-depth	CNOT-count	Depth	T-count	T-depth	CNOT-count	Depth	CNOT-count	%Diff.	Depth	%Diff.
Adder_8	24	19	399	69	466	223	215	15	1040	380	654	−37%	171	−55%
barenco_tof_10	19	9	224	96	224	288	100	32	396	314	216	−45%	196	−38%
barenco_tof_3	5	3	28	12	28	36	16	4	77	58	40	−48%	29	−50%
barenco_tof_4	7	4	56	24	56	72	28	8	124	99	66	−47%	52	−47%
barenco_tof_5	9	4	84	36	84	108	40	12	174	144	90	−48%	76	−47%
csla_mux_3	15	7	70	21	90	67	62	4	404	211	229	−43%	57	−73%
csum_mux_9	30	25	196	18	196	59	84	3	532	166	293	−45%	55	−67%
cycle_17_3	35	3	4739	2001	4742	5974	1944	522	6913	5303	4952	−28%	3897	−27%
GF(2^{10})_mult	30	211	700	108	709	290	410	2	4597	1095	2643	−43%	72	−93%
GF(2^{16})_mult	48	623	1792	180	1837	489	1040	2	12090	2538	8357	−31%	101	−96%
GF(2^{32})_mult	96	2527	7168	372	7292	1001	4128	2	98111	17660	42134	−57%	157	−99%
GF(2^{4})_mult	12	24	112	36	115	99	68	2	446	147	303	−32%	46	−69%
GF(2^{5})_mult	15	52	175	48	179	130	115	2	863	238	487	−44%	45	−81%
GF(2^{6})_mult	18	66	252	60	257	163	150	2	1009	272	792	−22%	57	−79%
GF(2^{7})_mult	21	128	343	72	349	195	217	2	1855	489	1109	−40%	58	−88%
GF(2^{8})_mult	24	128	448	84	469	233	264	2	2123	548	1590	−25%	72	−87%
GF(2^{9})_mult	27	210	567	96	575	258	351	2	2709	544	2181	−19%	69	−87%
grover_5	9	3	336	144	336	457	154	44	575	535	363	−37%	360	−33%
ham15-high	20	10	2457	996	2500	3026	1019	262	4285	3295	2656	−38%	1864	−43%
ham15-low	17	3	161	69	259	263	97	20	608	414	342	−44%	185	−55%
ham15-med	17	4	574	240	616	750	230	53	1087	788	636	−41%	423	−46%
hwb6	7	4	105	45	131	152	75	13	375	285	225	−40%	139	−51%
mod5_4	5	4	28	12	32	41	16	3	77	68	45	−42%	32	−53%
mod_adder_1024	28	6	1995	831	2005	2503	1011	230	3871	2614	2683	−31%	1675	−36%
mod_adder_1048576	58	10	17290	7292	17310	21807	7298	1879	29315	20154	20808	−29%	13875	−31%
mod_mult_55	9	4	49	15	55	50	35	4	147	87	84	−43%	47	−46%
mod_red_21	11	4	119	48	122	158	73	15	308	252	163	−47%	117	−54%
qcla_adder_10	36	39	238	24	267	73	162	6	924	219	457	−51%	65	−70%
qcla_com_7	24	17	203	27	215	81	94	7	489	172	280	−43%	79	−54%
qcla_mod_7	26	22	413	66	441	197	237	14	1153	352	669	−42%	150	−57%
qft_4	5	3	69	48	48	142	67	38	134	203	71	−47%	133	−34%
rc_adder_6	14	4	77	33	104	104	47	11	212	133	138	−35%	81	−39%
tof_10	19	3	119	51	119	153	71	17	287	221	158	−45%	111	−50%
tof_3	5	3	21	9	21	27	15	3	63	56	36	−43%	28	−50%
tof_4	7	3	35	15	35	45	23	5	101	91	56	−45%	39	−57%
tof_5	9	3	49	21	49	63	31	7	147	126	70	−52%	51	−60%
vbe_adder_3	10	6	70	24	80	79	24	5	116	71	75	−35%	43	−39%
Mean difference												−40.11%		−57.86%
Best savings												−57%		−99%
Worst savings												−19%		−27%

operators each of these three cost functions were able to uniquely return the shallowest circuits. So we cannot remove one of them. Furthermore, the fact that DaCSynth almost never returned the best result is a sign that we never had to synthesize worst case operators. Even for circuits acting on a large number of qubits (the Galois field multiplier GF(2^{32}) on 96 qubits for instance) the DaCSynth algorithm was not able to back off.

2) RESULTS WITH ANCILLARY QUBITS

We now repeat the experiment with the use of ancillary qubits. For each function, we let Tpar compute the number of ancillary qubits necessary to reduce the T-depth to its minimum. Then again we resynthesize each chunk of purely CNOT circuits. This time due to the use of ancillary qubits we need to synthesize some operators $A \in F_2^{p\times n}$, where n is the number of qubits and $p = n +$ #ancillas. To do the synthesis of one CNOT circuit, we have two options as follows.

1) Either computing the actual CNOT operator implemented by the CNOT circuit given by the Tpar algorithm, this is the "direct" method.
2) Or we can use our block algorithm described in Section V; this is the "block" method.

Note that even if $p < 2n$ the two methods are not equivalent because in the "block" method we compute the global operator differently (see our explanation in Section V).

So for each CNOT subcircuit, we did the synthesis twice, one with each method, and we kept the best result. We had to be careful about the size of the operators to synthesize. For some reversible functions the total number of qubits exceeds several hundreds and some of our methods cannot compute a solution in a reasonable amount of time. So for those extreme cases, we had to remove the greedy methods and even the DaCSynth algorithm for the Galois field multiplier in GF(2^{32}) for which the total number of qubits reaches more than 2500. Note that these restrictions only concern the "direct" method as the "block" method manages to synthesize only operators on at most $2n$ qubits. We consider it to be an asset of the "block" method over the "direct" synthesis.

The results are given in Table V. The statistics of the circuit output by the Tpar algorithm are shown, and we give the CNOT count and total depth after applying our optimizations. Again the savings compared to the Tpar circuits

are given. Overall we have even better savings than in the ancilla-free case. In average, we reduce the depth by almost 60%. The Galois field multipliers again give the best savings with up to 99% for the multiplier GF(2^{32}). As a bonus the total number of CNOT gates has also significantly decreased.

The performance frequency of each algorithm is given in Table VI. Again only the greedy methods with the cost functions H_{sum}, h_{prod}, and H_{prod} were useful. We also add the number of times the "block" and "direct" methods were the only method to return the best result. When the number of ancillary qubits is small, the direct method has to be privileged. This is probably due to our process to compute the global operator in the "block" method that is not efficient, this should be the subject of a future work. When the number of ancillas increase then the block method is more efficient, notably because the greedy methods do not scale well (both in terms of computational time and circuit size) when the problem size is too large.

VII. DISCUSSION AND FUTURE WORK

We see two main areas for improvements as follows.

1) First, from a practical point of view, it seems possible to improve the synthesis algorithm when the number of encoded ancillas is not more than n. The number of ancillas is not large enough to deploy a block strategy and we proposed a naive way to compute one operator that can "do the job" and that we can directly synthesize. However, the benchmarks have revealed that the operator already given by the Tpar algorithm is most of the time a better one.
2) Second, it seems clear when looking at the benchmarks that the upper bound of DaCSynth is to be improved. It is easy to have some results when we only consider the maximum number of ones in each row of $B = A_3A_1^{-1} \in F_2^{n\times n}$, but combining this with a restriction on the columns makes the proofs harder. For instance, it is easy to prove that one can flip no more than $n/2$ entries on each row of B to get a matrix $B \oplus C$ with only two different row vectors. Such matrix can be zeroed in a logarithmic number of steps and this would give an upper bound of approximately $n +$ logarithmic terms, which is closer to our benchmarks. Yet we are unable to get any property on the maximum number of 1 in the columns of C to conclude.

We now sketch some ideas of optimizations that could be candidates for improving our framework. In Section V, we showed that the implementation of an operator $A \in F_2^{p\times n}$, $p > n$, is in fact as costly as the synthesis of a square operator of size $k \leq 2n$ up to logarithmic terms. We want to highlight that this result can lead to new strategies for our initial divide-and-conquer framework and improve the theoretical upper bounds on the depth. Consider the matrix $B = A_3A_1^{-1} \in F_2^{n\times n}$ to zero during step 2 of the framework. If B is of rank $k < n$ then we write

$$B = DF$$

where $D \in F_2^{n\times k}$, $F \in F_2^{k\times n}$ are both of rank k. By using the block extension algorithm, we know that there is a sequence $(E_{i_D j_D})_{i_D j_D}$, respectively, $(E_{i_F j_F})_{i_F j_F}$), of row, respectively, column, operations of depth $\mathcal{O}(k)$ such that

$$\prod_{i_D, j_D} E_{i_D, j_D} D = \begin{pmatrix} I_k \\ 0 \end{pmatrix} F \prod_{i_F, j_F} E_{i_F, j_F} \qquad = \begin{pmatrix} I_k & 0 \end{pmatrix}.$$

Equivalently

$$\prod_{i_D, j_D} E_{i_D, j_D} B \prod_{i_F, j_F} E_{i_F, j_F} = \begin{pmatrix} I_k & 0 \\ 0 & 0 \end{pmatrix}$$

and B can be zeroed with a sequence of operations of depth $\mathcal{O}(k)$. So instead of trying to minimize the number of ones in B, as we do, one might be interested in diminishing the rank. The problem can be formulated as: given an integer $r < n$ and $B \in F_2^{n\times n}$ of rank $k > r$, what is the sequence of operations (row operations, column operations, entry flips) of minimum depth that transform B into a matrix of rank r?

This problem is related to other problems in the literature. The matrix rigidity of a matrix A is defined as the minimum Hamming distance between A and a matrix of rank r. In other words, the matrix rigidity of A is the number of entries of A that must be modified in order for the rank to drop to r. In the literature, the concept of matrix rigidity was used to prove lower bounds on the complexity of classical linear circuits [27], [28]. Most of the work we found on the subject was thus dedicated to finding explicit rigid matrices, which is quite the opposite of our approach. Moreover the distance for the matrix rigidity is defined as the number of flips in A whereas we are concerned in the depth of a sequence of operations.

The problem of matrix rigidity can be extended with the more general problem of low rank approximations, where we try to find, for given target rank r, the solution to

$$\min_{\text{rank}(R)=r} \|A - R\|$$

where $\|\cdot\|$ is an appropriate norm. Using the L_1 norm and we have the problem of finding the matrix rigidity of A. But again none of the norms usually considered take into account the depth required to implement R. Finally, such problems only consider one of the three operations that are available to us, namely the entry flips. Although row and column operations alone cannot reduce the rank of a matrix, they can help in creating a new matrix that needs less entries to flip to have a reduced rank.

Finally, can we extend DaCSynth to take into account connectivity constraints? We believe, it will be complicated because it is not natural in a restricted connectivity to split the qubits into two sets, especially if there is no particular symmetry between the two sets. We think, it is preferable to

TABLE VI Frequency of Best Performance of Each Algorithm During the Optimization of Reversible Circuits With the Use of Ancillary Qubits. For Each Algorithm, the First Column Gives the Number of Times It Has Returned the Best Result (Possibly Other Algorithms Returned Circuits of Same Size). When Available, the Second Column Reports the Number of Times It Was the Only One to Provide the Best Possible Circuit. When There is Only One Column, It Was Never the Only One to Provide the Best Possible Circuit

Function	$\#n$	#Block	#Direct	#CNOT sub-circuits	Kutin et al	DaCSynth	Greedy (H_{sum}, size)	Greedy (h_{prod}, size)	Greedy (H_{sum})		Greedy (h_{prod})		Greedy (H_{prod})		LU + Greedy (H_{sum})	LU + Greedy (H_{prod})
					Best choice	Best Choice	Best choice	Best choice	Best choice	Only Choice	Best choice	Only Choice	Best choice	Only Choice	Best choice	Best choice
Adder_8	43	0%	49%	59	18 (31%)	5 (8%)	30 (51%)	28 (47%)	44 (75%)	3 (5%)	38 (64%)	1 (2%)	34 (58%)	0 (0%)	26 (44%)	26 (44%)
barenco_tof_10	28	1%	23%	101	57 (56%)	39 (39%)	85 (84%)	85 (84%)	87 (86%)	0 (0%)	87 (86%)	0 (0%)	86 (85%)	0 (0%)	70 (69%)	70 (69%)
barenco_tof_3	8	0%	70%	24	8 (33%)	4 (17%)	10 (42%)	9 (38%)	10 (42%)	0 (0%)	10 (42%)	0 (0%)	10 (42%)	0 (0%)	9 (38%)	8 (33%)
barenco_tof_4	11	5%	38%	35	16 (46%)	9 (26%)	19 (54%)	19 (54%)	21 (60%)	0 (0%)	21 (60%)	0 (0%)	19 (54%)	0 (0%)	16 (46%)	16 (46%)
barenco_tof_5	13	0%	31%	46	25 (54%)	14 (30%)	30 (65%)	30 (65%)	32 (70%)	0 (0%)	32 (70%)	0 (0%)	30 (65%)	0 (0%)	25 (54%)	25 (54%)
csla_mux_3	22	0%	27%	11	1 (9%)	1 (9%)	3 (27%)	3 (27%)	6 (55%)	0 (0%)	10 (91%)	5 (45%)	5 (45%)	0 (0%)	1 (9%)	2 (18%)
csum_mux_9	55	0%	0%	23	1 (4%)	3 (13%)	3 (13%)	3 (13%)	9 (39%)	2 (9%)	6 (26%)	0 (0%)	5 (22%)	0 (0%)	2 (9%)	2 (9%)
cycle_17_3	38	0%	5%	1410	582 (41%)	450 (32%)	892 (63%)	853 (60%)	1374 (97%)	1 (0%)	1169 (83%)	15 (1%)	1273 (90%)	1 (0%)	826 (59%)	817 (58%)
GF(2^{10})_mult	241	67%	0%	42	1 (2%)	1 (2%)	2 (5%)	2 (5%)	14 (33%)	4 (10%)	16 (38%)	8 (19%)	15 (36%)	3 (7%)	2 (5%)	2 (5%)
GF(2^{16})_mult	671	83%	0%	58	1 (2%)	1 (2%)	1 (2%)	1 (2%)	19 (33%)	10 (17%)	22 (38%)	16 (28%)	18 (31%)	5 (9%)	1 (2%)	1 (2%)
GF(2^{32})_mult	2623	100%	0%	100	1 (1%)	1 (1%)	1 (1%)	1 (1%)	15 (15%)	3 (3%)	56 (56%)	48 (48%)	35 (35%)	18 (18%)	1 (1%)	1 (1%)
GF(2^{4})_mult	36	17%	0%	12	2 (17%)	2 (17%)	3 (25%)	2 (17%)	10 (83%)	1 (8%)	10 (83%)	2 (17%)	6 (50%)	0 (0%)	2 (17%)	2 (17%)
GF(2^{5})_mult	67	33%	33%	10	2 (20%)	2 (20%)	4 (40%)	3 (30%)	7 (70%)	0 (0%)	9 (90%)	3 (30%)	5 (50%)	0 (0%)	2 (20%)	2 (20%)
GF(2^{6})_mult	84	50%	17%	28	2 (7%)	2 (7%)	1 (4%)	1 (4%)	9 (32%)	2 (7%)	8 (29%)	4 (14%)	7 (25%)	1 (4%)	3 (11%)	3 (11%)
GF(2^{7})_mult	149	33%	33%	12	1 (8%)	1 (8%)	1 (8%)	1 (8%)	4 (33%)	0 (0%)	11 (92%)	5 (42%)	7 (58%)	0 (0%)	1 (8%)	1 (8%)
GF(2^{8})_mult	152	33%	17%	33	1 (3%)	1 (3%)	2 (6%)	1 (3%)	12 (36%)	2 (6%)	13 (39%)	5 (15%)	11 (33%)	0 (0%)	1 (3%)	1 (3%)
GF(2^{9})_mult	237	83%	0%	40	1 (2%)	1 (2%)	4 (10%)	4 (10%)	17 (42%)	4 (10%)	14 (35%)	4 (10%)	17 (42%)	2 (5%)	2 (5%)	2 (5%)
grover_5	12	0%	9%	130	66 (51%)	57 (44%)	115 (88%)	106 (82%)	116 (89%)	1 (1%)	115 (88%)	0 (0%)	114 (88%)	0 (0%)	88 (68%)	87 (67%)
ham15-high	30	1%	22%	745	395 (53%)	263 (35%)	628 (84%)	602 (81%)	737 (99%)	21 (3%)	684 (92%)	6 (1%)	641 (86%)	1 (0%)	524 (70%)	519 (70%)
ham15-low	20	2%	34%	56	18 (32%)	7 (12%)	47 (84%)	44 (79%)	51 (91%)	2 (4%)	54 (96%)	5 (9%)	38 (68%)	0 (0%)	25 (45%)	24 (43%)
ham15-med	21	0%	35%	151	73 (48%)	41 (27%)	134 (89%)	124 (82%)	150 (99%)	3 (2%)	141 (93%)	1 (1%)	121 (80%)	0 (0%)	95 (63%)	94 (62%)
hwb6	11	0%	30%	51	15 (29%)	10 (20%)	34 (67%)	28 (55%)	35 (69%)	1 (2%)	33 (65%)	2 (4%)	31 (61%)	0 (0%)	19 (37%)	17 (33%)
mod5_4	9	0%	40%	10	8 (80%)	7 (70%)	9 (90%)	8 (80%)	10 (100%)	1 (10%)	9 (90%)	0 (0%)	8 (80%)	0 (0%)	8 (80%)	8 (80%)
mod_adder_1024	34	0%	6%	687	360 (52%)	242 (35%)	487 (71%)	474 (69%)	663 (97%)	0 (0%)	633 (92%)	3 (0%)	611 (89%)	1 (0%)	449 (65%)	436 (63%)
mod_adder_1048576	68	0%	1%	5459	2644 (48%)	1888 (35%)	3607 (66%)	3537 (65%)	5268 (97%)	6 (0%)	4727 (87%)	71 (1%)	4903 (90%)	4 (0%)	3367 (62%)	3350 (61%)
mod_mult_55	109	9%	18%	11	5 (45%)	2 (18%)	7 (64%)	5 (45%)	10 (91%)	1 (9%)	8 (73%)	0 (0%)	10 (91%)	0 (0%)	5 (45%)	4 (36%)
mod_red_21	15	0%	44%	50	21 (42%)	7 (14%)	34 (68%)	32 (64%)	36 (72%)	0 (0%)	33 (66%)	0 (0%)	30 (60%)	0 (0%)	27 (54%)	28 (56%)
qcla_adder_10	75	6%	24%	31	5 (16%)	4 (13%)	9 (29%)	7 (23%)	16 (52%)	1 (3%)	12 (39%)	0 (0%)	15 (48%)	0 (0%)	7 (23%)	7 (23%)
qcla_com_7	41	0%	35%	34	8 (24%)	4 (12%)	15 (44%)	14 (41%)	17 (50%)	1 (3%)	16 (47%)	0 (0%)	16 (47%)	2 (6%)	9 (26%)	9 (26%)
qcla_mod_7	48	8%	16%	51	9 (18%)	5 (10%)	26 (51%)	17 (33%)	32 (63%)	3 (6%)	24 (47%)	0 (0%)	26 (51%)	3 (6%)	13 (25%)	13 (25%)
qft_4	105	0%	43%	23	15 (65%)	10 (43%)	11 (48%)	11 (48%)	23 (100%)	0 (0%)	23 (100%)	0 (0%)	20 (87%)	0 (0%)	9 (39%)	9 (39%)
rc_adder_6	18	0%	49%	51	25 (49%)	21 (41%)	33 (65%)	32 (63%)	37 (73%)	0 (0%)	35 (69%)	0 (0%)	34 (67%)	0 (0%)	29 (57%)	29 (57%)
tof_10	22	0%	48%	56	24 (43%)	17 (30%)	40 (71%)	38 (68%)	42 (75%)	0 (0%)	41 (73%)	0 (0%)	39 (70%)	0 (0%)	34 (61%)	34 (61%)
tof_3	105	0%	50%	8	4 (50%)	2 (25%)	2 (25%)	2 (25%)	8 (100%)	0 (0%)	7 (88%)	0 (0%)	5 (62%)	0 (0%)	2 (25%)	2 (25%)
tof_4	10	0%	58%	26	2 (8%)	2 (8%)	10 (38%)	9 (35%)	12 (46%)	0 (0%)	11 (42%)	0 (0%)	8 (31%)	0 (0%)	7 (27%)	7 (27%)
tof_5	12	0%	59%	31	9 (29%)	5 (16%)	15 (48%)	13 (42%)	17 (55%)	0 (0%)	16 (52%)	0 (0%)	15 (48%)	0 (0%)	14 (45%)	15 (48%)
vbe_adder_3	16	7%	7%	29	6 (21%)	4 (14%)	13 (45%)	12 (41%)	14 (48%)	1 (3%)	14 (48%)	1 (3%)	12 (41%)	0 (0%)	9 (31%)	8 (28%)

improve the results from [14] for the LNN architecture and extend it to an arbitrary topology.

VIII. CONCLUSION

We have proposed DaCSynth, a scalable algorithm for synthesizing shallow linear reversible quantum circuits and we have shown that synthesizing an operator with a divide-and-conquer algorithm is equivalent to zeroing binary matrices with three elementary operations. This gives a framework that generalizes other works and widens the perspective of finding new techniques. We have derived an upper bound that improves existing bounds for registers of intermediate sizes and we have used a greedy algorithm to obtain the shallowest possible circuits. In our benchmarks, the circuits produced by the algorithm DaCSynth have a depth, which is twice smaller than state-of-the-art algorithms. We have also presented purely greedy algorithms providing close to optimal results for small or simple operators. Applied to the synthesis of a class of reversible functions, we report some substantial savings in the total depth of the circuits while keeping the T-depth as low as possible. This article represents one step toward the compilation of quantum circuits that can be executed on a quantum hardware in the future. As future work, we will study how to adapt this method to take into account the connectivity constraints between the qubits in real hardware. Another future work will be to extend DaCSynth to Clifford circuits. Syntheses of Clifford circuits through normal forms are possible (see, e.g., [29]–[31]), but it would also be interesting to see if DaCSynth has an equivalent in the symplectic group $Sp(2n, \mathbb{F}_2)$ used to represent Clifford operators with a different set of elementary operations available. An interesting result would be to see if a direct synthesis can produce better depths rather than using normal forms.

APPENDIX A
KUTIN ET AL'S ALGORITHM FOR LNN CONNECTIVITY: PRESENTATION AND EXTENSION TO FULL QUBIT CONNECTIVITY

Kutin *et al.* gave several constructions of specific linear reversible operations for the LNN architecture: addition, swap, permutation, generic linear reversible operator [14]. They focused on the shallowest way to do it. For a generic linear reversible operator, they relied on their construction for reversing the qubits, i.e., the image of an n-qubit state $|x_1x_2\ldots x_n\rangle$ is $|x_nx_{n-1}\ldots x_1\rangle$. This construction is a *sorting network* and contains only SWAP gates (see Fig. 7). The network, as a SWAP circuit, is of depth n. An example with seven qubits is given in Fig. 8. Then they considered the same sorting network but with *boxes* replacing the SWAP gates. Each box, acting on 2 qubits, can perform one of the following operations:

1) $(u, v) \to (u, v)$, requiring 0 CNOT;
2) $(u, v) \to (u, u \oplus v)$, requiring 1 CNOT;
3) $(u, v) \to (u \oplus v, v)$, requiring 1 CNOT;
4) $(u, v) \to (v, u \oplus v)$, requiring 2 CNOT;

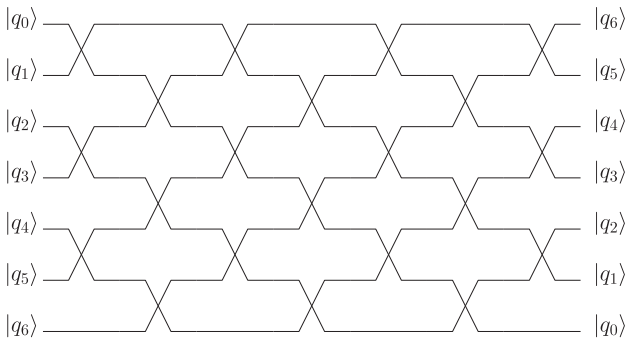

FIG. 7. Sorting network for 7 qubits. As a SWAP circuit, the depth of the circuit is *n*. Replacing each SWAP by a box gives a skeleton circuit for the synthesis of triangular linear reversible operators.

5) $(u, v) \to (u \oplus v, u)$, requiring 2 CNOT;
6) $(u, v) \to (v, u)$, requiring 3 CNOT.

Kutin *et al.* [14] proved that a sorting network made of boxes can transform any operator into a northwest triangular one. Moreover, for each box, only the state of one of the two output qubits needs to be fixed after applying the box. This means that we can always choose a box that needs at most two CNOTs to be implemented. Consequently, the total depth of the sorting network is $2n$. Finally, they showed how to synthesize a northwest triangular operator with a similar sorting network except that in this case for each box the states of the two output qubits need to be fixed. Therefore, we may need at most three CNOTs for some boxes (if we only need to swap the qubits) and the depth of this second part is upper bounded by $3n$. Overall this gives a generic method for synthesizing any linear reversible operator for the LNN architecture in depth at most $5n$. To our knowledge, this is the best result in the literature for the case of restricted connectivity. This result can only be improved by a constant factor as Kutin *et al.* also showed that some operators need at least circuits with depth $2n$ to be implemented. So the best possible synthesis method for the LNN architecture should provide circuits of depth comprised between $2n$ and $5n$. For other architectures, the bounds are not clear. Obviously, if an architecture contains a Hamiltonian path in it then one can apply the algorithm for the LNN case, giving an upper bound of $5n$ for the depth. To our knowledge, lower bounds are not known but Maslov computed lower bounds for two simplified models in the case where each qubit has k neighbors [17]. The first model is the case where we have to execute every gate given by the Gaussian elimination algorithm in a given order; the second model is less restrictive as we have to execute every gate, but we assume that they all commute. In both cases, the depth is lower bounded linearly in n.

A. EXTENSION TO FULL QUBIT CONNECTIVITY

Although it was not done in their paper, the algorithm proposed by Kutin *et al.* [14] can be extended to the full connectivity case: this is what we show in this paragraph. To our

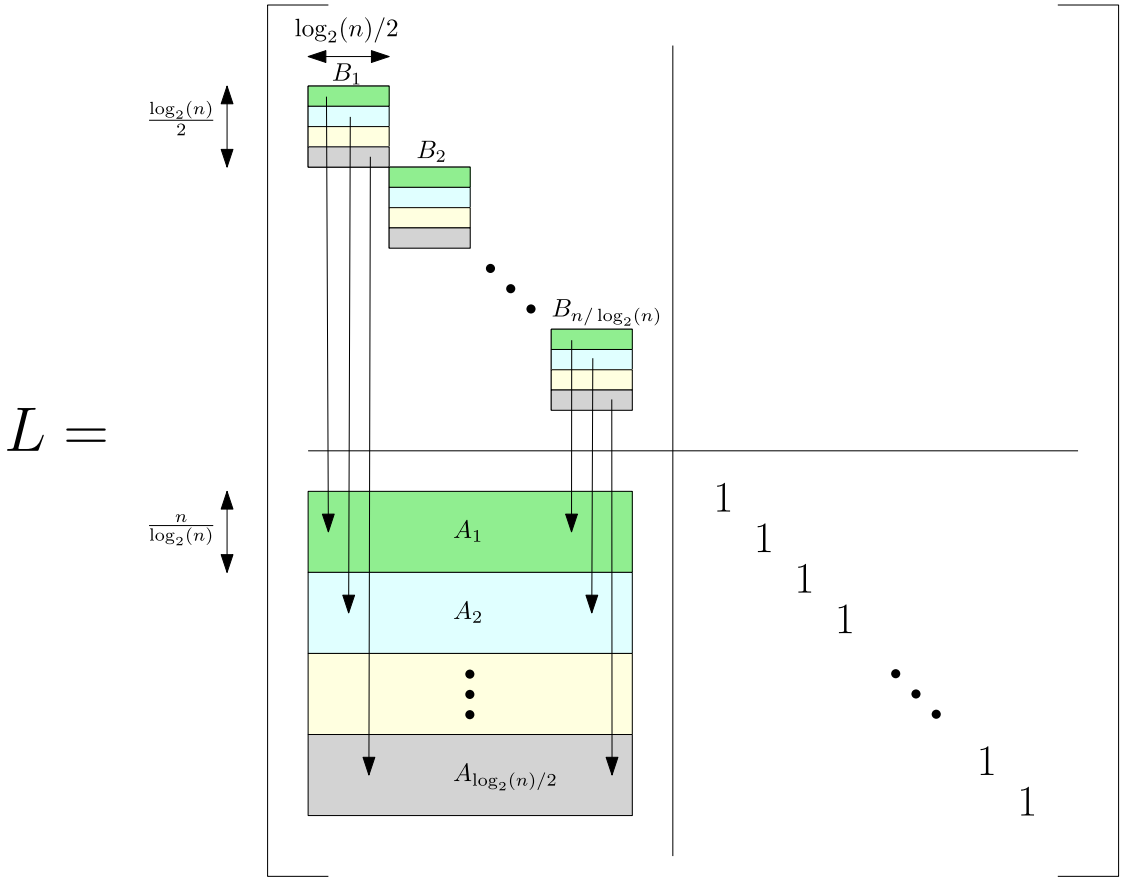

FIG. 8. **Block structure of the triangular operator *L* for Jiang *et al.*'s algorithm.**

knowledge, such an extension has never been proposed in the literature.

In the original Kutin *et al.*'s algorithm [14], each box corresponds to an interaction between a pair of qubits and it can be decomposed into two parts: first, we execute the interaction strictly speaking between the two qubits with a CNOT gate, secondly, we move the qubits in the hardware by swapping them. If we consider that the connectivity is full then we do not need to move the qubits anymore in the hardware. This means that we can replace each box by a CNOT gate and we get rid of the SWAP gates. We end with a new skeleton circuit that is functionally equivalent to the one given by Kutin *et al.* except that each box is now a single CNOT. The skeleton circuit from Kutin *et al.*, as a box-based circuit, is of depth $2n$. Therefore, our new skeleton, as a CNOT-based circuit, is also of depth $2n$. To our knowledge, this was the best result until the asymptotically optimal algorithm proposed recently in [15]. The pseudocode of this new algorithm is given Algorithm 1. For simplicity, we only show the case for a lower triangular operator, the generalization to any operator is done via an LU decomposition [32]

$$A = PLU$$

where A is the operator to synthesize, P is a permutation matrix, and L, respectively, U, are lower, respectively, upper, triangular operators. With full qubit connectivity, a permutation can be implemented with a circuit of constant depth 6 [33]. Each triangular operator can be synthesized with a circuit of depth n, leading to a total depth of $2n + 6$ for the synthesis of an arbitrary operator. Given that we do not move the qubits anymore, most of the algorithm consists in tracking what would be the positions of the qubits in the hardware to determine, which interactions need to be done at a given time step. Then, it is easy to decide if, for a given pair of qubits (i, j), a CNOT gate needs to be added. If the operator is lower triangular, we only have to decide if we add the CNOT $(i \to j)$, $i < j$ as we must not ruin the triangular structure by adding a CNOT $(j \to i)$. Then, if the ith component of the jth row is one then add a CNOT $(i \to j)$. The reason why it works is not straightforward: we have to note that when we decide to apply or not a CNOT $(i \to j)$, either the components $k < i$ have already been treated for qubit i so it cannot modify the components of qubit j, or such components have not been treated on both qubits, so modifying them on qubit j is not a problem as they will be zeroed later in the algorithm.

APPENDIX B
JIANG ET AL.'S ALGORITHM

The authors propose an algorithm based on the LU decomposition and a divide-and-conquer approach. The proof of

Algorithm 1 Adaptation of Kutin *et al.*'s algorithm [14] on a triangular operator L for a full qubit connectivity.

Require: $n \geq 0$, $L \in \mathbb{F}_2^{n\times n}$ triangular
Ensure: C is a CNOT-circuit implementing L with depth at most n

```
C ← [ ]
perm ← [[1, n]]
for j = 1 to n do
 if j ≡ 1[2] then
   start ← 1
 else
   start ← 2
 end if
 while start < n do
   if L[perm[start+1], perm[start]] = 1 then
     C.append(CNOT(perm[start], perm[start+1]))
   end if
   perm[start], perm[start+1] ← perm[start+1],
   perm[start]
   start ← start + 2
 end while
end for
return reverse(C)
```

the optimal depth complexity is quite hard to summarize but the principle of the algorithm is simpler so we give a brief description of it. First, the algorithm starts with an LU decomposition $A = PLU$. Again P can be synthesized in constant depth six, therefore, we only need to treat the triangular case. We illustrate with the lower triangular case. The synthesis of L consists in a divide-and-conquer algorithm, the operator L is decomposed as

$$L = \begin{pmatrix} L_{\lfloor n/2\rfloor} & \\ A & L_{\lceil n/2\rceil} \end{pmatrix}$$

where $L_{\lfloor n/2\rfloor}$ and $L_{\lceil n/2\rceil}$ are triangular operators of size $\lfloor n/2\rfloor$ and $\lceil n/2\rceil$, respectively, and A is any Boolean matrix of size $\lfloor n/2\rfloor \times \lceil n/2\rceil$. The algorithm initially synthesizes in parallel both triangular suboperators by applying recursively the algorithm. Then, we are left with the operator

$$L' = \begin{pmatrix} I & \\ A' & I \end{pmatrix}$$

to synthesize. This is done by considering the following blocks in L:

1) the northwest identity operator is seen as a block diagonal operator with $n/\log_2(n)$ blocks of size $\log_2(n)/2$, noted $B_1, \ldots, B_{n/\log_2(n)}$;
2) A is divided into $\log_2(n)/2$ blocks of $n/\log_2(n)$ rows, noted $A_1, \ldots, A_{\log_2(n)/2}$. For simplicity, we consider each A_i as a matrix $C_i \in (F_2^{\log_2(n)/2})^{\frac{n}{\log_2(n)}\times\frac{n}{\log_2(n)}}$, i.e., we see A_i as a $\frac{n}{\log_2(n)} \times \frac{n}{\log_2(n)}$ matrix with elements from $F_2^{\log_2(n)/2}$.

The specific structure of L is summarized in Fig. 8. The synthesis of L consists in successive applications of the following two stages of row operations:

1) row operations on the B_i's such that specific words of $\log_2(n)/2$ bits appear on each row;
2) row operations between the B_i's and the A_i's to zero words of $\log_2(n)/2$ bits of A.

More precisely, the kth row of a B_i has to zero the ith column of C_k. For that a sequence of operators on $\log_2(n)/2$ qubits is computed such that the property "Every word on $\log_2(n)/2$ bits appears on each row of the B_i's" is verified. Such sequence of operators is called a row traversal sequence. The operators of the row traversal sequence are computed in parallel on each B_i via the row operations during Stage 1. Once we have the desired operator on each B_i, we need to compute the appropriate row operations of Stage 2. Each row of a B_i act on a specific C_k so the corresponding row operations can be done in parallel. So all we need is to see how to coordinate the row operations acting on the same C_k. For simplicity consider the case $k = 1$, i.e., all the first rows of each B_i are used to zero C_1. Given that all B_i's are identical, the choice of applying a row operation from block B_i to the kth row of C_1 is: is $C[k, i]$ equal to $B_*[1, :]$ (where the index on B has been omitted to emphasize that all B_i's are the same)? Therefore the matrix C_1 can be seen as the adjacency matrix P of a bipartite graph G where $P[k, i] = 1$ if $C_1[k, i] = B_*[1, :]$. A sequence of parallel row operations between the B_i's and C_1 corresponds to a matching in G and a "good" sequence of parallel row operations is given by a matching decomposition of G. A central theorem that we will also use in our own work is the following: if the maximum number of 1 in a row or a column of P is p then there exists a decomposition of G into p matchings, i.e., a sequence of p parallel row operations is necessary to zero all the entries of C equal to $B_*[1, :]$. Given that each word appears on each row of the B_i's we are ensured that A will be zero at the end of the algorithm. Finally, we need to assume that A is sufficiently random, if it is not the case one can decompose $A = A' \oplus A''$ with $A,' A''$ sufficiently random and do the process two times, the first time for adding A' and the second time for adding A''.

The depth $d(n)$ for the synthesis of one triangular operator is, therefore, given by

$$d(n) = d(n/2) + 2 \times \text{ length row traversal sequence} \times \left(\underbrace{d(\log_2(n))}_{\text{synthesize the operator } B_i} + \text{size matching decomposition} \right). \quad (4)$$

Finally the authors have shown that the length of the row traversal sequence is $\mathcal{O}(\sqrt{n})$ and if A is sufficiently random at each iteration the matching decomposition is of size

$\mathcal{O}(\sqrt{n}/\log_2(n))$. Therefore

$$d(n) = d(n/2) + \mathcal{O}(\sqrt{n}) \times (d(\log_2(n)) + \mathcal{O}(\sqrt{n}/\log_2(n)))$$
$$= \alpha(n/\log_2(n)) + \beta(\sqrt{n}/\log_2(n)))$$

hence, the result.

Let us now compute an estimation for α, β. As a divide-and-conquer framework, the authors have derived a recursive formula in the case of triangular operators. Noting $d(n)$ for the depth, we have

$$d(n) \leq d(n/2) + 2 \times \mathcal{O}(\sqrt{n}) \times (\mathcal{O}(\log_2(n)) + \mathcal{O}(\sqrt{n}/\log_2(n))).$$

Note that we think there is a typo in their formula, the term $\mathcal{O}(\log_2(n))$ being $\mathcal{O}(\log^3{}_2(n))$ in their paper. This term corresponds to the synthesis of an operator of size $\log_2(n)/2$. Assuming that we use the best algorithm, i.e., the adaptation of Kutin *et al.*'s algorithm [14] we proposed in Appendix A, each of these operators can be synthesized with a circuit of depth at most $2 \times \log_2(n)/2 = \log_2(n)$. We may have missed something but this improves the real complexity so we keep our proposed modification. The second term $\mathcal{O}(\sqrt{n}/\log_2(n)))$ corresponds to the matching decomposition of a graph and the authors showed that the leading coefficient is $\sqrt{e}$. The third term, $\mathcal{O}(\sqrt{n})$, corresponds to the length of the row-traversal sequence on k qubits that gives a sequence of k-qubit operators such that for any bitstring of size k and any integer $j \in [\![1, k]\!]$, there is an operator in the sequence whose jth row equals the bitstring. The authors proved that there exists a row-traversal sequence on k qubits of length $3 \times 2^{k-1} - k + 1$. Here, we have $k = \log_2(n)/2$ and $\mathcal{O}(\sqrt{n}) = 3/2 \times \sqrt{n}$. Therefore, we finally get

$$d(n) \leq d(n/2) + 3 \times \sqrt{n} \times \left(\log_2(n) + \sqrt{ne}/\log_2(n)\right)$$
$$\leq d(n/2) + 3\sqrt{n}\log_2(n) + 3\frac{n\sqrt{e}}{\log_2(n)}$$

and

$$d(n) \leq 3 \times \left(\sum_{j=0}^{\log_2(n)-1} \sqrt{\frac{n}{2^j}} \log_2\left(\frac{n}{2^j}\right) + \frac{\sqrt{e}\frac{n}{2^j}}{\log_2\left(\frac{n}{2^j}\right)} \right).$$

After simplification, we have

$$d(n) \leq 3 \times \left(2\sqrt{e}\frac{n}{\log_2(n)} + 3.3\sqrt{n}\log_2(n)\right)$$

and we have to do it for the two triangular operators given by the LU decomposition. Overall

$$\text{depth [15]} \leq 20\left(\frac{n}{\log_2(n)} + \sqrt{n}\log_2(n)\right).$$

Although it is only an upper bound, in practice there is little simplification one can make when synthesizing a specific operator: the row-traversal sequence still needs to be synthesized entirely and the matching decomposition is done on random graphs so we cannot expect the exact complexity to be that lower compared to the upper bound.

REFERENCES

[1] F. Arute *et al.*, "Quantum supremacy using a programmable superconducting processor," *Nature*, vol. 574, no. 7779, pp. 505–510, 2019, doi: 10.1038/s41586-019-1666-5

[2] H.-S. Zhong *et al.*, "Quantum computational advantage using photons," *Science*, vol. 370, pp. 1460–1463, 2020, doi: 10.1126/science.abe8770.

[3] E. Pednault, J. Gunnels, D. Maslov, and J. Gambetta, "On quantum supremacy." [Online]. Available: https://www.ibm.com/blogs/research/2019/10/on-quantum-supremacy/

[4] S. Aaronson, "Chinese bosonsampling experiment: The gloves are off." [Online]. Available: https://www.scottaaronson.com/blog/?p=5159

[5] S. Bravyi and A. Kitaev, "Universal quantum computation with ideal clifford gates and noisy ancillas," *Phys. Rev. A*, vol. 71, Feb. 2005, Art. no. 022316, doi: 10.1103/PhysRevA.71.022316

[6] L. E. Heyfron and E. T. Campbell, "An efficient quantum compiler that reduces t count," *Quantum Sci. Technol.*, vol. 4, no. 1, Sep. 2018, Art. no. 015004, doi: 10.1088/2058-9565/aad604

[7] M. Amy and M. Mosca, "T-count optimization and reed-muller codes," *IEEE Trans. Inf. Theory*, vol. 65, no. 8, pp. 4771–4784, Aug. 2019, doi: 10.1109/TIT.2019.2906374.

[8] A. Kissinger and J. van de Wetering, "Reducing the number of non-clifford gates in quantum circuits," *Phys. Rev. A*, vol. 102, Aug. 2020, Art. no. 022406, doi: 10.1103/PhysRevA.102.022406

[9] F. Zhang and J. Chen, "Optimizing t gates in clifford t circuit as $\pi/4$ rotations around paulis," 2019, *arXiv:1903.12456*.

[10] M. Amy, D. Maslov, and M. Mosca, "Polynomial-time t-depth optimization of clifford t circuits via matroid partitioning," *IEEE Trans. CAD Integr. Circuits Syst.*, vol. 33, no. 10, pp. 1476–1489, Oct. 2014, doi: 10.1109/TCAD.2014.2341953.

[11] D. Maslov, "Optimal and asymptotically optimal nct reversible circuits by the gate types," *Quantum Inf. Comput.*, vol. 16, no. 13/14, pp. 1096–1112, 2016, doi: 10.26421/QIC16.13-14-2.

[12] M. Amy, P. Azimzadeh, and M. Mosca, "On the controlled-NOT complexity of controlled-NOTphase circuits," *Quantum Sci. Technol.*, vol. 4, no. 1, Sep. 2018, Art. no. 015002, doi: 10.1088/2058-9565/aad8ca.

[13] D. Gottesman, "Stabilizer codes and quantum error correction," Ph.D. dissertation, California Inst. Technol., Pasadena, CA, USA, 1997. [Online]. Available: https://arxiv.org/abs/quant-ph/9705052

[14] S. A. Kutin, D. P. Moulton, and L. Smithline, "Computation at a distance," *Chicago J. Theor. Comput. Sci.*, vol. 2007, 2007. [Online]. Available: http://cjtcs.cs.uchicago.edu/articles/2007/1/contents.html

[15] J. Jiang, X. Sun, S. Teng, B. Wu, K. Wu, and J. Zhang, "Optimal space-depth trade-off of CNOT circuits in quantum logic synthesis," in *Proc. ACM-SIAM Symp. Discrete Algo.*, Salt Lake City, UT, USA, Jan. 5–8, 2020, pp. 213–229, doi: 10.1137/1.9781611975994.13.

[16] K. N. Patel, I. L. Markov, and J. P. Hayes, "Optimal synthesis of linear reversible circuits," *Quantum Inf. Comput.*, vol. 8, no. 3, pp. 282–294, 2008, doi: 10.26421/QIC8.3-4-4.

[17] D. Maslov, "Linear depth stabilizer and quantum fourier transformation circuits with no auxiliary qubits in finite-neighbor quantum architectures," *Phys. Rev. A*, vol. 76, Nov. 2007, Art. no. 052310, doi: 10.1103/PhysRevA.76.052310.

[18] A. Kapoor and R. Rizzi, "Edge-coloring bipartite graphs," *J. Algorithms*, vol. 34, no. 2, pp. 390–396, 2000, doi: 10.1006/jagm.1999.1058.

[19] F. Freibert, "The classification of complementary information set codes of lengths 14 and 16," *Adv. Math. Commun.*, vol. 7, no. 3, pp. 267–278, 2013, doi: 10.3934/amc.2013.7.267.

[20] J. Edmonds, "Paths, trees, and flowers," *Can. J. Math.*, vol. 17, pp. 449–467, 1965, doi: 10.4153/CJM-1965-045-4.

[21] L. Klein, "Combinatorial optimization with one quadratic term," Doctoral dissertation, Tech. Univ. Dortmund, Fakultät für Math., Vienna, Austria, 2014.

[22] T. G. de Brugière, M. Baboulin, B. Valiron, S. Martiel, and C. Allouche, "Gaussian elimination versus greedy methods for the synthesis of linear reversible circuits," *ACM Trans. Quantum Comput.*, to be published, doi: 10.1145/3474226.

[23] M. Amy, "Matthew Amy's Github." [Online]. Available: https://github.com/meamy

[24] J. Bezanson, A. Edelman, S. Karpinski, and V. B. Shah, "Julia: A fresh approach to numerical computing," *SIAM Rev.*, vol. 59, no. 1, pp. 65–98, 2017, doi: 10.1137/141000671.

[25] Y. Nam, N. J. Ross, Y. Su, A. M. Childs, and D. Maslov, "Automated optimization of large quantum circuits with continuous parameters," *NPJ Quantum Inf.*, vol. 4, no. 1, 2018, Art. no. 23, doi: 10.1038/s41534-018-0072-4.

[26] N. J. Ross, "J. Neil Ross's Github." [Online]. Available: https://github.com/njross

[27] L. G. Valiant, "Graph-theoretic arguments in low-level complexity," in *Proc. 6th Symp. Math. Found. Comput. Sci.*, Tatranska Lomnica, Czechoslovakia, Sep. 5–9, 1977, pp. 162–176, doi: 10.1007/3-540-08353-7_135

[28] S. V. Lokam, "Complexity lower bounds using linear algebra," *Found. Trends Theor. Comput. Sci.*, vol. 4, no. 1/2, pp. 1–155, 2009, doi: 10.1561/0400000011.

[29] D. Maslov and M. Roetteler, "Shorter stabilizer circuits via bruhat decomposition and quantum circuit transformations," *IEEE Trans. Inf. Theory*, vol. 64, no. 7, pp. 4729–4738, Jul. 2018, doi: 10.1109/TIT.2018.2825602.

[30] S. Aaronson and D. Gottesman, "Improved simulation of stabilizer circuits," *Phys. Rev. A*, vol. 70, Nov. 2004, Art. no. 052328, doi: 10.1103/PhysRevA.70.052328.

[31] R. Duncan, A. Kissinger, S. Perdrix, and J. Van De Wetering, "Graph-theoretic simplification of quantum circuits with the ZX-calculus," *Quantum*, vol. 4, p. 279, 2020, doi: 10.22331/q-2020-06-04-279.

[32] G. H. Golub and C. F. Van Loan, *Matrix Computations*, 3rd ed. Baltimore, MD, USA: Johns Hopkins Univ. Press, 1996.

[33] C. Moore and M. Nilsson, "Parallel quantum computation and quantum codes," *SIAM J. Comput.*, vol. 31, no. 3, pp. 799–815, 2001, doi: 10.1137/S0097539799355053.